Sveriges lantbruksuniversitet
Swedish University of Agricultural Sciences

Department of Energy and Technology

# Energy analysis of a fruit drying plant in Adeiso, Ghana

Ambjörn Lätt & Tomas Löfwall

Projektarbete i energisystem 2014:1
Civilingenjörsprogrammet i energisystem

Uppsala 2014

SLU, Swedish University of Agricultural Sciences
Faculty of Natural Resources and Agricultural Sciences
Department of Energy and Technology

Ambjörn Lätt & Tomas Löfwall

Energy analysis of a fruit drying plant in Adeiso, Ghana

Supervisor: Cecilia Sundberg, institutionen för energi och teknik, SLU
Assistant supervisor: Maik Blaser, HPW Fresh & Dry Ltd, Adeiso, Ghana
Examiner: Johan Vinterbäck, institutionen för energi och teknik, SLU
Assistant examiner: Sven Smårs, institutionen för energi och teknik, SLU
TE0012, Project Work in Energy Systems Engineering15 credits, Technology, Advanced A1N
Master Programme in Energy Systems Engineering (Civilingenjörsprogrammet i energisystem) 300 credits

Series title: Projektarbete i energisystem, institutionen för energi och teknik, SLU
2014:1

Uppsala 2014

Keywords: energy analysis, fruit drying, Minor Field Study, Ghana, biogas, solar, renewable energy

Online publication: http://stud.epsilon.slu.se

Cover: The roof of HPW Fresh & Dry factory, with solar panels and heat storage tank, 2013. Photo: Tomas Löfwall

# Abstract

The purpose of the project has been to work out recommendations that reduce the energy-related costs and environmental impact of HPW Fresh & Dry Ltd., a fruit drying factory in Ghana. The factory produces electricity with diesel and biogas but also purchases electricity from the national electricity company. Heat for the drying process is produced from biogas, kerosene and solar panels. In the project the energy system was analyzed by measuring production and consumption of heat and electricity.

The project results show that the factory can become self-sufficient on heat if the available energy is used more efficient. The production units for both electricity and heat have low efficiencies. Inadequate insulation and sealing contributes to the poor performance of the heat system. The electricity measurements show that several electrical loads are unbalanced and that the three phase cooling machines are not fully utilized.

The factory is recommended to invest in a new kerosene boiler and a roaster boiler for combustion of coconut waste. Furthermore, the biogas should be combusted in a boiler instead of in the now used combined heat and power engine (CHP), for improved utilization of the gas. Unused capacity of the three phase cooling machines could replace the less efficient single-phase cooling machines. Moreover, the electrical loads should be balanced and the usage of motors connected to the biogas plant minimized. By insulating pipings and seal leakages, heat losses and the need of cooling will decrease. Finally, the factory is recommended to install automatic regulation of the boilers to avoid over-heating of the storage tank.

# Sammanfattning

Syftet med projektet har varit att ta fram rekommendationer för hur HPW Fresh & Dry Ltd., en frukttorkningsfabrik i Ghana, kan minska sina energirelaterade kostnader och sin miljöpåverkan. Fabriken producerar el med diesel och biogas samt köper el från nationella elbolaget. Värme till torkprocessen produceras med biogas, fotogen och solpaneler. I projektet analyserades energisystemet genom att mäta produktion och konsumtion av värme och el.

Resultaten från projektet visar att fabriken kan bli självförsörjande på värme om den tillgängliga energin används mer effektivt. Produktionsenheterna för både el och värme generellt har låga verkningsgrader. Bristfällig isolering och tätning bidrar till den låga prestandan i värmesystemet. Elmätningarna visar bland annat att flera elektriska laster är obalanserade samt att det finns outnyttjad kylkapacitet i fabrikens trefasiga kylmaskiner.

Fabriken rekommenderas att investera i en ny fotogenvärmepanna samt en värmepanna för förbränning av kokosnötavfall. Vidare bör biogasen förbrännas i en värmepanna istället för i den nu använda kraftvärmemotorn, för att bättre utnyttja gasen. Outnyttjad kylkapacitet på de trefasiga kylmaskinerna kan ersätta mindre effektiva enfasiga kylmaskinerna. Dessutom bör de elektriska lasterna balanseras och driften av elmotorer till biogasanläggningen minimeras. Genom att isolera rör och täta värmeläckage kan värmeförluster och kylbehov minskas. Slutligen rekommenderas fabriken att installera automatisk reglering av värmepannorna för att undvika övervärmning av ackumulatortanken.

## Acknowledgements

First and foremost we would like to express our greatest gratitude to Maik Blaser, Managing Director of HPW Fresh & Dry Ltd., for his daily engagement in the project, his hospitality and our late dinner discussions.

Cecilia Sundberg, Associate Professor at SLU and our supervisor, deserves special thanks for her establishment of necessary contacts in Ghana, project startup guidance and valuable comments on the report.

We would also like to thank:

Philip Yaw Moro, Bright Keme, Frank Gomado and the rest of the technical staff for their assistance in our daily work and their patience with our disturbing measurements.

Angela Essandoh Araba for helping us with the recordings of processed fruit during the dryer measurements.

Maria Forsberg and Johanna Grim, for laying the foundation of the cooperation with HPW Fresh & Dry through their excellent work on the biogas plant.

Dr. Johan Abrahamsson at Uppsala University, for his generosity with the lending of measurement equipment and for valuable tips on electricity measurements.

Kent Almstrand at Wallox Elektronik AB, for enabling the delivery of the heat energy meter with short notice, and for valuable tips on the heat measurements.

# Abbreviations

| Abbreviation | Description |
|---|---|
| **CHP** | Combined Heat and Power |
| **COP** | Coefficient Of Performance |
| **CSV** | Comma Separated Values |
| **ECG** | Electricity Company of Ghana Limited |
| **EROI** | Energy Return On Investment |
| **GHC** | Ghana Cedi (currency) |
| **HHV** | Higher Heating Value |
| **KNUST** | Kwame Nkrumah University of Science and Technology |
| **LPG** | Liquid Petroleum Gas |
| **MFS** | Minor Field Study |
| **PV** | Photo Voltaic |
| **RMS** | Root Mean Square |
| **Sida** | Swedish International Development Cooperation Agency |
| **SLU** | Swedish University of Agricultural Sciences |
| **STC** | Standard Test Conditions |

# Table of Content

# 1 Introduction

In Adeiso, sixty kilometers outside of Accra, the Swiss company HPW Fresh & Dry limited runs a fruit drying factory since the year of 2011. The factory process 6500 tons of fresh fruit into 470 tons of finished products annually. The main products are dried pineapple, mango, banana and coconut. The factory employs 400 workers and provides market for 100 farmers or farmer organizations (Blaser 2013).

The factory uses kerosene, solar panels and a biogas combined heat and power engine (CHP) for heat supply. Electricity is produced by a diesel generator and the biogas CHP but also purchased from the national electricity company. The company strives towards becoming energy self-sufficient, and as a part of the work an energy audit has been requested with the purpose of finding possible energy savings. The collaboration between the HPW Fresh & Dry fruit factory and SLU was established the year of 2012 when Johanna Grim and Maria Johansson did a minor field study on the factory's biogas plant (Grim and Johansson 2012). The cooperation was successful and both parties were very satisfied with the results and experiences.

The factory manager Mr. Maik Blaser describes the factory as a patch work, meaning that the plant has been built bit by bit, lacking system perspective. Furthermore, the factory has expanded significantly in a short time. The expansion is likely to continue, increasing the need of efficient energy usage.

The project was carried out in the form of a Minor Field Study, i.e. as an eight week study in the country with part financing through scholarships from the Swedish International Development Agency (Sida). The study was performed by Ambjörn Lätt and Tomas Löfwall at HPW Fresh & Dry Ltd. in Adeiso, Ghana during the period 22$^{nd}$ October 2013 to 10$^{th}$ January 2014. The project and this report was conducted within the scope of the course Project Work in Energy Systems Engineering (15 credits), which is an eligible course of the Master Programme in Energy Systems Engineering at Uppsala University and SLU.

# 2 Purpose and Question

The purpose of the project is to find profitable energy savings at the HPW Fresh & Dry fruit factory in Adeiso, Ghana. The proposed energy saving measures should also reduce the environmental impact. Furthermore, to achieve continuity in the company's energy efficiency work the staff will be trained throughout the project.

Question: How can HPW Fresh & Dry reduce their energy-related costs?

# 3 Project Workplan

The project was divided into the following partial projects:

1. Draw rough sketches of the factory's heat and electricity system
2. Test the measurement equipment
3. Measure production of heat from the
   - 3.1. Solar panels
   - 3.2. Biogas CHP motor
   - 3.3. Kerosene boiler
   - 3.4. Heat recovery from water cooled air condition
   - 3.5. Heat recovery from fruit dryers
4. Measure consumption of heat from the
   - 4.1. Fruit dryers
   - 4.2. Biogas plant
5. Measure heat losses from pipings
6. Measure/read electricity production from the
   - 6.1. National grid
   - 6.2. Diesel generator
   - 6.3. Biogas CHP motor
7. Measure electricity consumption of the
   - 7.1. Four main loads
     - 7.1.1. Old factory
     - 7.1.2. Dryers
     - 7.1.3. New factory
     - 7.1.4. Overhead line
   - 7.2. Fruit dryers
   - 7.3. Biogas plant
   - 7.4. Cooling system
8. Measure/read the fuel consumption of
   - 8.1. Biogas
   - 8.2. Kerosene
   - 8.3. Diesel
9. Propose energy efficiency measures
10. Interchange and training with the factory staff
11. Process and analyze data
12. Write report
13. Present the project

# 4 System Description

## 4.1 Electricity System

An overview of the factory's electricity system is shown in figure 4.1. Not all switching combinations are possible since the biogas CHP is the only generator capable of synchronizing with the national grid (ECG).

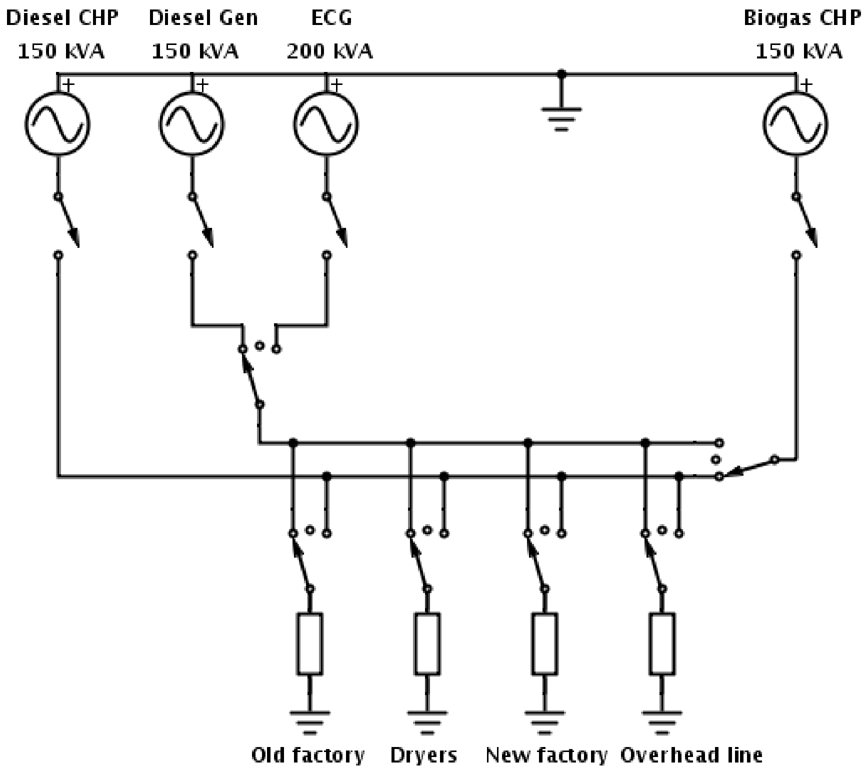


**Figure 4.1: Sketch of the factory's electricity system**

The electricity system of the factory can be supplied by four different sources:

1. The national grid via an 11 kV overhead line, through an 11 kV/400 V, 200 kVA transformer (denoted ECG and shown in figure 4.2).
2. A 150 kVA generator manufactured by CAT, run by a Perkins diesel engine (denoted diesel generator and shown in figure 4.2).
3. A 150 kVA combined heat and power generator manufactured by Camda Generator Works, run by a biogas engine (denoted biogas CHP and shown in figure 4.2).
4. A 150 kVA combined heat and power generator manufactured by Camda Generator Works, run by a diesel engine (denoted diesel CHP). The generator is malfunctioning.

In practice, the upper load limit for the biogas CHP is around 60 kVA. The diesel generator can deliver approximately 90 kVA.

**Figure 4.2: Transformer, diesel generator (yellow) and biogas CHP (red)**

There are four main loads connected to the supply lines (figure 4.3):

1. Old factory: Supplies the older part of the factory including cooling, office, canteen, lab and laundry, but also the circulation pumps for dryer 1-3.
2. Dryers: Supplies fans, louvers and automation of all four fruit dryers.
3. New factory: Supplies the newer part of the factory including cooling and the fruit shredder for the biogas plant.
4. Overhead line: Supplies pumps, mixers and stirrers for the biogas plant as well as pumps for the bore holes.

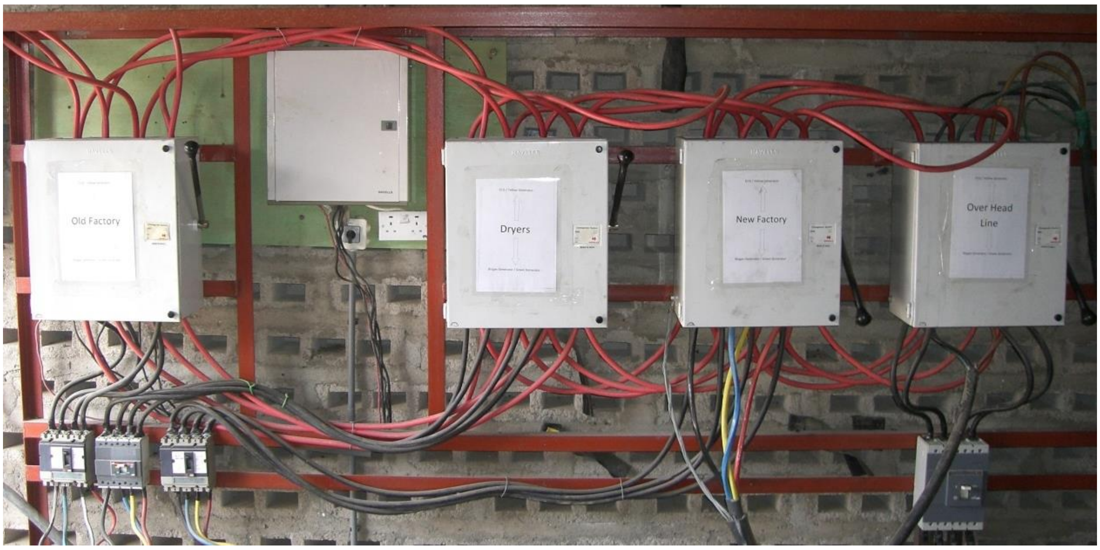


**Figure 4.3: Electrical main loads. From left: Old factory, Dryers, New factory, Overhead line**

## 4.2 Heat System

An overview of the factory's heat system is depicted in figure 4.4.

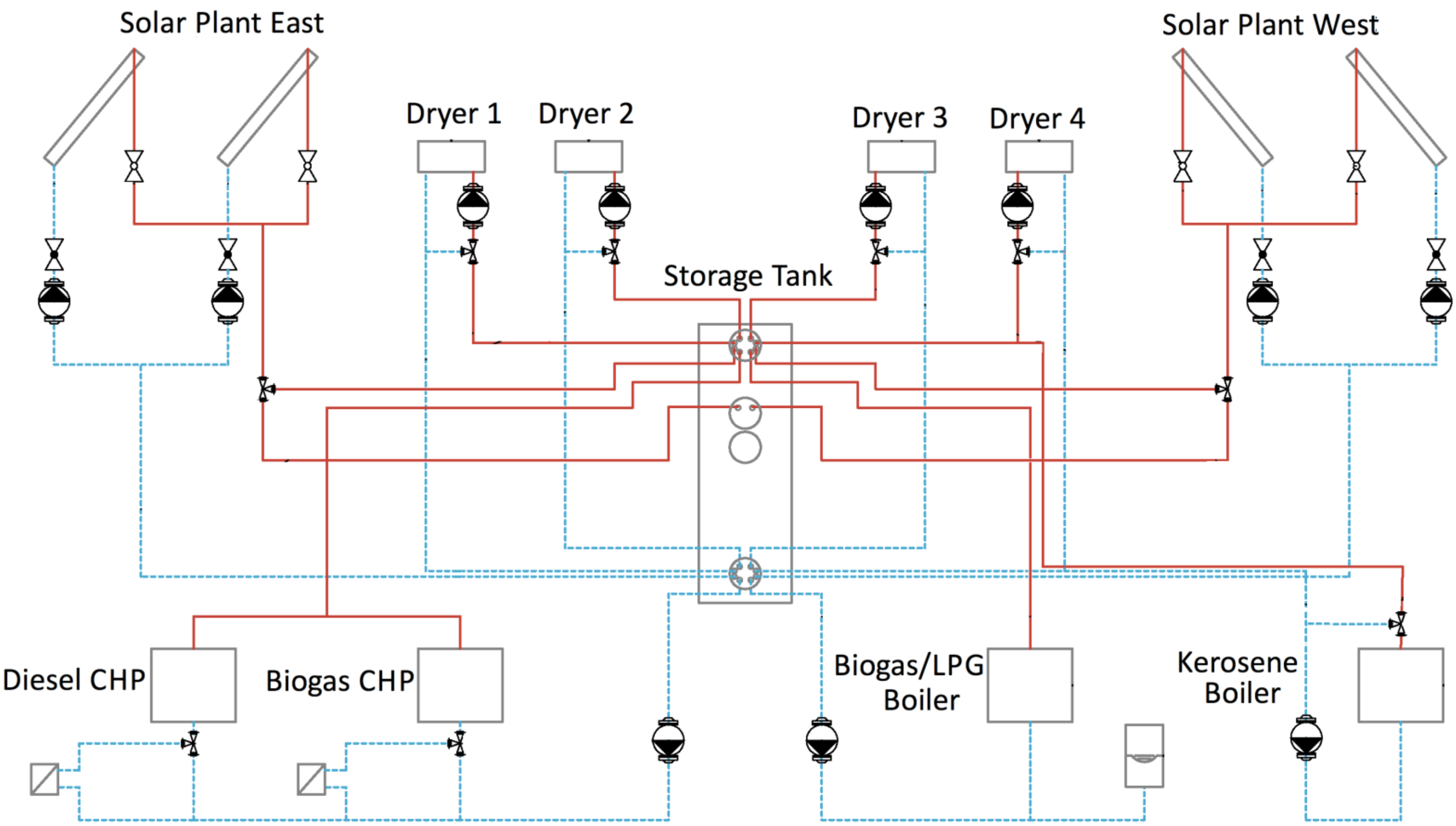


**Figure 4.4: Sketch of the factory's heat system. Modified drawing from solar plant corporate promoter (Junod 2013)**

Four producers supply the heat system:

1. The biogas CHP (figure 4.2). Recovers heat from two heat exchangers, one connected to the water-cooling system of the engine and one connected the exhaust pipe.
2. The solar plant (figure 4.5). Installed on the factory's roof and consists of 315 panels, 160 on the west side and 145 on the east side. The total panel area is 580 $m^2$ and the absorber area is 545 $m^2$ (Guangdong 2011).
3. The kerosene boiler (figure 4.5). Has a capacity of 600 $kW_{thermal}$.


**Figure 4.5: Heat storage tank, kerosene boiler and solar panels**

In addition there are two production units that are malfunctioning, a diesel CHP and a boiler for biogas and liquid petroleum gas (LPG).

There are two loads in the heat system:

1. The fruit dryers. Dryer 1-3 are of the same type and rated 200 $kW_{thermal}$ each while dryer 4 is rated 540 kW. All four dryers recover heat from the exhaust to the inlet through two air/water heat exchangers.
2. The biogas plant (figure 4.6). The fermentation tanks are supplied with heat from the water cooled cooling machine in order to keep an optimum fermentation temperature of 35-37 °C (Grim and Johansson 2012:36).

**Figure 4.6: Fermenters and gas storage balloons of the biogas plant**

All producing units and the four dryers are connected to a 40 $m^3$ heat storage tank (figure 4.5). The supply pipes from all producing units and to all consuming units are connected to the top of the tank. In addition, half of the supply pipes from the solar plant is connected to the middle of the tank, giving the solar plant a higher utilization since it allows a wider supply temperature range. The return pipes to all producing units and from all consuming units are connected to the bottom of the tank.

The circulation pumps of the solar plant system are regulated by temperature sensors connected to the top of the solar panels and to the bottom of the storage tank. The pumps start when the temperature difference between the panels and tank bottom exceeds 6 °C, and shuts off when the temperature difference is less than 3 °C.  The utilization of the solar panels is therefore dependent on the bottom temperature of the storage tank. An additional temperature sensor measures the tank top temperature.

The kerosene boiler can deliver heat directly to dryer 4 while the excess heat is supplied to the storage tank, as implied by figure 4.4 and 4.5. The shunted circuit of the kerosene boiler circulates the water inside the boiler before the supply temperature exceeds 80 °C. At that point the shunt opens to let the heat flow to the consumers.

A shunted circuit is also utilized by the heat supply system of the dryers. The circulation pump is installed inside the circuit and is always running at maximum speed when the dryer is on. The supply temperature to the dryer is regulated by the shunt valve opening, allowing the right amount of heat to flow into the shunted circuit.

## 4.3 Cooling System

A sketch of the factory's cooled facilities is shown in figure 4.7. The sketch can also give an idea of the layout of the factory.

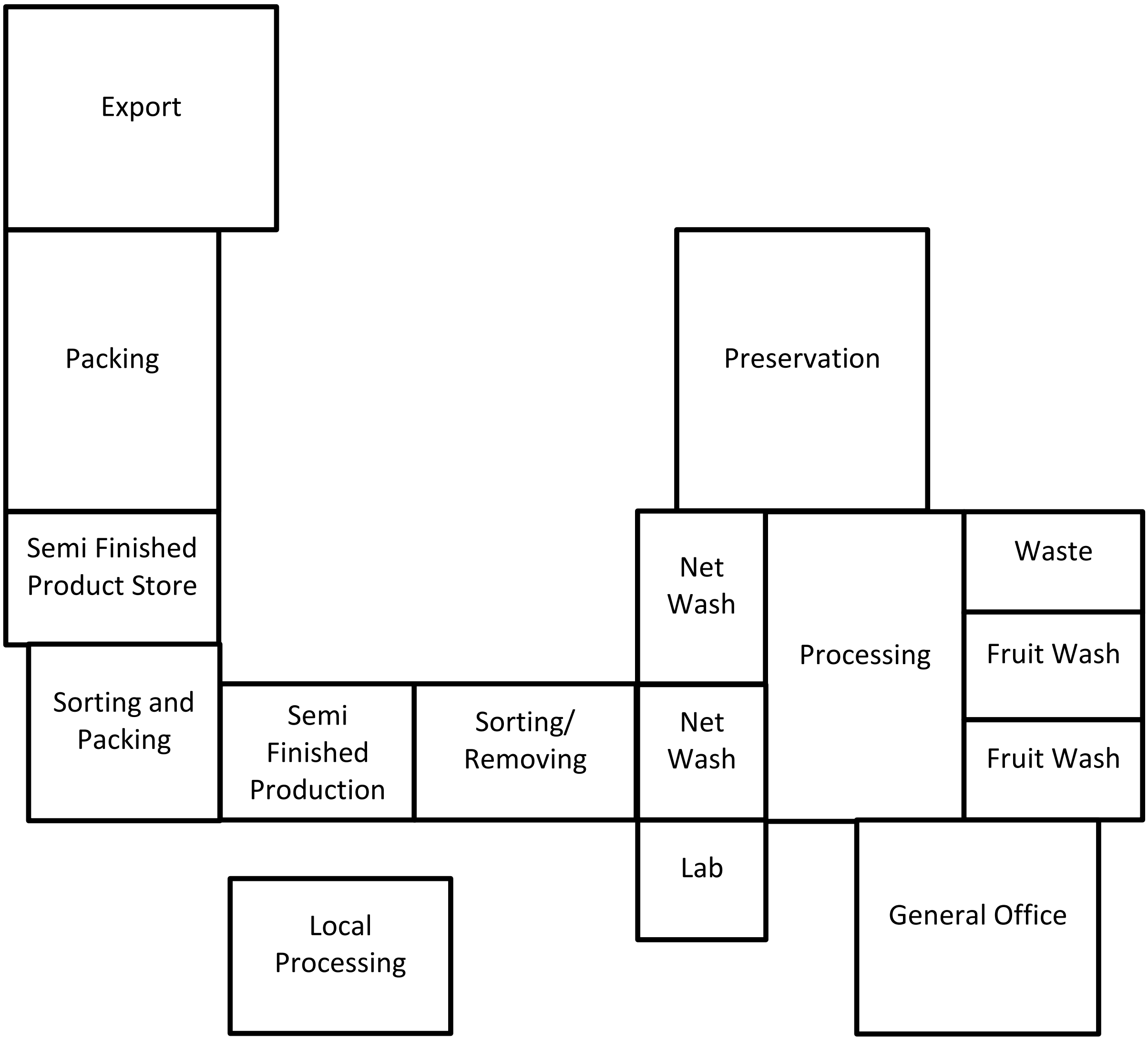


**Figure 4.7: Sketch of the factory's cooled facilities. The dryers are situated in the open space in the middle**

Table 4.1 shows the temperature and installed evaporator cooling capacity for the factory's cooled facilities together with the supplying compressors. The compressors are named after their maximum current rating.

**Table 4.1: Temperature and installed evaporator cooling capacity of the cooled facilities**

| Facility | Temp [°C] | Evap cooling capacity [kW] | Compressor |
|---|---|---|---|
| **Semi Finished Prod. Store** | 8 | 7.2 | Bitzer tandem 2*7.8 A |
| **Sorting and Packing** | 15 | 7.2 | Bitzer tandem 2*7.8 A |
| **Semi Finished Prod.** | 15 | 7.2 | Bitzer tandem 2*7.8 A |
| **Sorting/Removing** | 22 | 4.1 | Bitzer tandem 2*10.8 A |
| **Trays Washing** | 22 | 8.5 | Bitzer tandem 2*10.8 A |
| **Fruit Washing** | 22 | 7.1 | Bitzer tandem 2*10.8 A |
| **Waste** | 22 | 2.7 | Bitzer tandem 2*10.8 A |
| **Processing** | 22 | 29.4 | Bitzer 2*24.6 A |
| **Preservation** | 22 | 26 | Bitzer 2*24.6 A |
| **Packing** | 15 | 20.7 | Bitzer 2*24.6 A |
| **Export Room** | 8 | 18.4 | Bitzer 1*15.9 A |
| **Local Processing Room** | 22 | 7.8 | LG 12.5 A + LG 6.3 A |
| **Lab** | 24 | 5.2 | LG 12.5 A |
| **General Office** | 20 | 10.4 | 2*LG 12.5 A |

The following list describes the cooling machines:

- Bitzer tandem 2*7.8 A and 2*10.8 A are three phase compressors with air cooled condensers, each with two compressors on the same shaft. Their cooling capacities are 20.8 and 30.7 kW.
- Bitzer 2*24.6 A (figure 4.8) is a three phase machine with a water cooled condenser, two separate compressors and a cooling capacity of 61.6 kW. The cooling agent is R134a with a condensing temperature of 50 °C, and the manufacturer recommends a water inlet temperature of 30 °C. The recommended flow is 5 $m^3/h$ and the maximum capacity is 8 $m^3/h$. (Bitzer 2012)
- Bitzer 1*15.9 A (figure 4.8) is a three phase compressor with air cooled condenser and a cooling capacity of 17.8 kW.
- LG 12.5 A and 6.3 A are single phase compressors with air cooled condensers and cooling capacities of 5.2 and 2.6 kW.

The only facilities with nighttime cooling are the semi finished product store room and the export room. Hence only Bitzer tandem 2*7.8 A and Bitzer 1*15.9 A are running during the night.

Figure 4.8: Bitzer tandem 2*24.6 A (water cooled) atop and Bitzer 1*15.9 A (air cooled)

## 4.4 Biogas Plant

A sketch of the biogas plant can be seen in figure 4.9. The fermenters (figure 4.6) are heated by the cooling water from the condenser of Bitzer 2*24.6 A. An ABB TRIO-WIRL 40 gas flow meter is installed before the filter to measure the consumption of biogas.

The biogas plant is powered by motors according to table 4.2.

Table 4.2: Rated powers of the biogas plant's motors

| Motors | Rated power [kW] |
|---|---|
| **Shredder** | 7.5 |
| **Pump** | 10.5 |
| **Mixer** | 4.5 |
| **Stirrers** | 2*10.5 |

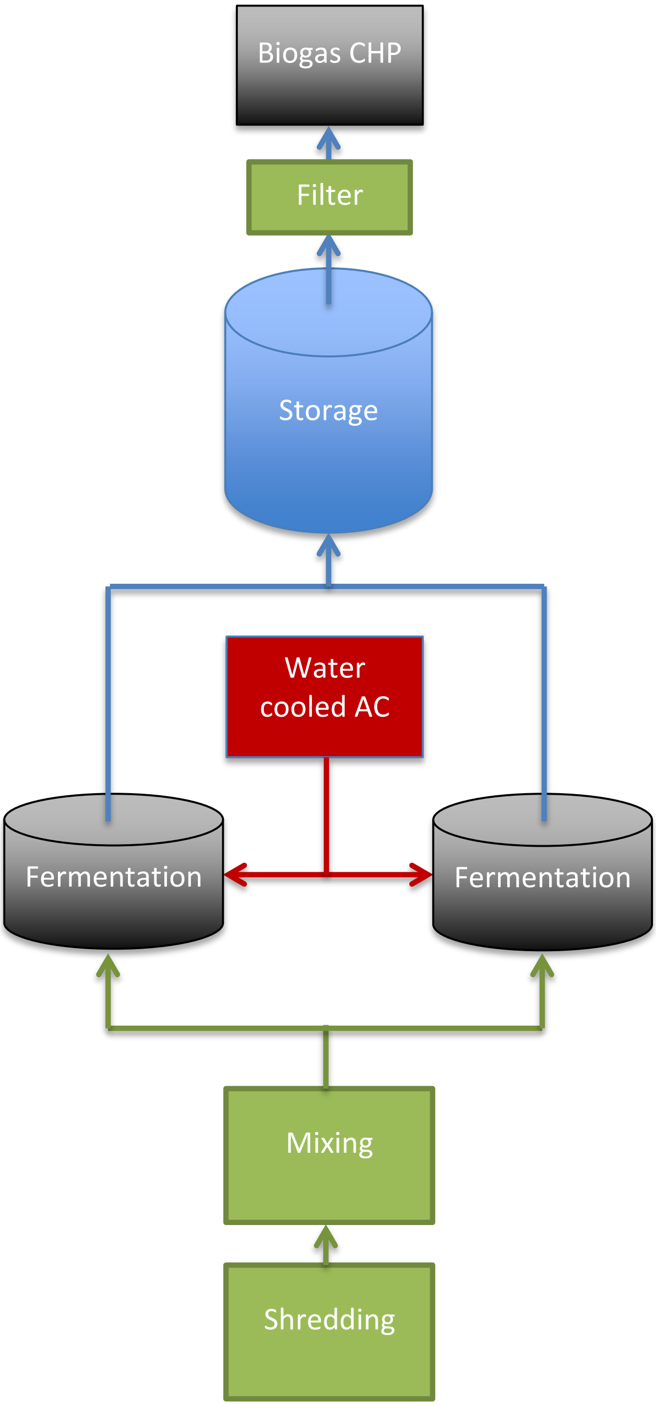


**Figure 4.9: Sketch of the factory's biogas plant**

# 5 Theory

## 5.1 Efficient Energy Usage

This chapter presents some useful principles for efficient usage of energy. In general, an efficient energy system converts and distributes energy with small losses. The efficiency of the production and consumption units should not only be considered alone but also as parts of the complete energy system. For example, heat produced by an efficient boiler is worth nothing if it does not reach the heat consumer. Hence sources of heat leakage, such as pipings and storage, should be minimized and insulated properly. Furthermore, when the main heat consumer has used the high-exergy heat the rest can sometimes be recovered or used or by other sources. Low-exergy heat can also be retrieved from the condensers of cooling machines. The electricity consumption of a cooling machine is reduced if the heat flow between the cooled facility and its surroundings is minimized. That is accomplished with a small temperature difference and sufficient insulation of the facility.

Another important aspect is dimensioning, i.e. to install equipment that is not larger than necessary. For example, the load of an electric generator should be close to the rated power for efficient running. The same holds for electric motors.

## 5.2 Electricity

### 5.2.1 Power in Three Phase Systems

When measuring power in three phase systems the following equations need to be considered.

The line-to-neutral voltages of phases a, b and c are shifted 120° between each other according to equations 5.1, 5.2 and 5.3.

$$V_{an} = V_{LN\,peak} * \sin(\omega t) \qquad [V] \qquad \text{Eq 5.1}$$
$$V_{bn} = V_{LN\,peak} * \sin(\omega t - 120°) \qquad [V] \qquad \text{Eq 5.2}$$
$$V_{cn} = V_{LN\,peak} * \sin(\omega t - 240°) \qquad [V] \qquad \text{Eq 5.3}$$

where $V_{LN\,peak}$ [V] is the peak value of the line-to-neutral voltage. The corresponding line-to-line voltages are shifted 30° compared to the line-to-neutral voltages according to equations 5.4, 5.5 and 5.6.

$$V_{ab} = \sqrt{3} * V_{LN\,peak} * \sin(\omega t + 30°) \qquad [V] \qquad \text{Eq 5.4}$$
$$V_{bc} = \sqrt{3} * V_{LN\,peak} * \sin(\omega t - 90°) \qquad [V] \qquad \text{Eq 5.5}$$
$$V_{ca} = \sqrt{3} * V_{LN\,peak} * \sin(\omega t - 210°) \qquad [V] \qquad \text{Eq 5.6}$$

The active power of one phase is given by equation 5.7.

$$P_{1\emptyset} = V_{LN}^{rms} * I^{rms} * \cos(\varphi) \qquad [W] \qquad \text{Eq 5.7}$$

where $V_{LN}^{rms}$ [V] and $I^{rms}$ [A] are the root-mean-square (rms) values of the line-to-neutral voltage and the current through one phase, cos(φ) is the power factor and φ is the phase difference between the current and voltage. The phase difference is caused by inductive and/or capacitive elements in a circuit. Since the factory uses many induction motors the current will normally lag the voltage. The phase difference will cause a reactive power flow that can be quantified by equation 5.8.

$$Q_{1\emptyset} = V_{LN}^{rms} * I^{rms} * \sin(\varphi) \quad [\text{VAr}] \qquad \text{Eq 5.8}$$

The apparent or complex power is the vector sum of active and reactive power but can also be calculated from equation 5.9.

$$S_{1\emptyset} = V_{LN}^{rms} * I^{rms\ conj} \quad [\text{VA}] \qquad \text{Eq 5.9}$$

where $I^{rms\ conj}$[A] is the conjugate of the rms value of the current through one phase.

### 5.2.2 Clamp-on Current Meter

A clamp-on current meter is a current transformer with the primary winding represented by the current carrying conductor placed inside the clamp. The iron clamp is attached to a secondary winding that reduces the current input to the meter (Fluke 2013: Fluke Clamp Meters)

By measuring the voltage and current simultaneously both active and reactive power can be calculated according to equation 5.7 and 5.8.

## 5.3 Heat

### 5.3.1 Thermal Power

The thermal power is calculated with equation 5.10,

$$\dot{Q}_{12} = \dot{m} * \bar{c} * (t_2 - t_1) \quad [\text{W}] \qquad \text{Eq 5.10}$$

where $\dot{m}$ [kg/s] is the mass flow, $\bar{c}$ [kJ/kg*K] is the specific heat capacity of the fluid and $t_2 - t_1$ [K] is the temperature difference over the heat sink/source (Alvarez, p.265). Since the heat capacity of water in liquid phase is almost constant, throughout the project it is assumed to be the value holding for 300 K, i.e. 4.2 kJ/kg*K (Nordling and Österman 2006:38).

### 5.3.2 Thermal Efficiency of the Solar Plant

The thermal efficiency of the solar plant is calculated with equation 5.11.

$$\eta_{Solar\ plant} = \frac{P_{Solar\ plant}/A_{Panels}}{P_{Irradiation}} \quad [-] \qquad \text{Eq 5.11}$$

where $P_{Solar\ plant}$ [W] is the thermal power delivered by the solar plant when the sun is shining, $A_{Panels}$ [m$^2$] is the panel absorption area of the measured plant section and $P_{Irradiation}$ [W/m$^2$] is the solar irradiance when the sun is shining. Since no on-site measurement of the irradiation is available a restrictive value of 1000 W/m$^2$ is assumed according to standard test conditions (STC).

### 5.3.3 Heat Losses from Pipes

The heat loss from a pipe is calculated with equation 5.12.

$$P = \alpha * \pi * D * \Delta t \qquad [\text{W/m}] \qquad \text{Eq 5.12}$$

where $\alpha$ [W/m$^2$*K] is the thermal conductivity, D [m] is the outer diameter of the pipe and $\Delta t$ is the temperature difference between the pipe's surface and the ambient air (Alvarez 2006:366). The thermal power loss is a sum of convection and radiation from the pipe (Alvarez 2006:391), giving equation 5.13 for thermal conductivity.

$$\alpha = \alpha_{conv} + \alpha_{rad} \qquad [\text{W/m}^2\text{*K}] \qquad \text{Eq 5.13}$$

where $\alpha_{conv}$ is described by Nusselt according to equation 5.14, holding for surface temperatures above 10 °C (Alvarez 2006:369).

$$\alpha_{conv} = 2.6 * \Delta t^{0.25} \qquad [\text{W/m}^2\text{*K}] \qquad \text{Eq 5.14}$$

$\alpha_{rad}$ is calculated with equation 5.15.

$$\alpha_{rad} = \varepsilon_{res} * C_s * \beta \qquad [\text{W/m}^2\text{*K}] \qquad \text{Eq 5.15}$$

where $\varepsilon_{res}$is the emissions ratio, which is 0.61, i.e. equal the emissions ratio for steel (Alvarez 2006:389). $C_s$=5.67 [$\frac{W}{m^2\left(\frac{K}{100}\right)^4}$] is the black body radiation constant, and $\beta$ is a variable described by equation 5.16.

$$\beta = \frac{\left(\frac{T_1}{100}\right)^4 - \left(\frac{T_2}{100}\right)^4}{T_1 - T_2} \qquad [\text{-}] \qquad \text{Eq 5.16}$$

where $T_1$ and $T_2$ [K] are the surface and ambient temperatures. (Alvarez 2006:389)

### 5.3.4 Estimation of Heat Production from the Solar Plant

The estimation of daily heat production from the solar plant is calculated with equation 5.17.

$$E_{Solar\ plant} = E_{Irradiation} * A_{Panels} * \eta_{Solar\ plant} \qquad [\text{kWh}] \qquad \text{Eq 5.17}$$

where $E_{Irradiation}$ [kWh/m$^2$*day] is the daily average of irradiated solar energy estimated for Adeiso to 5 kWh/m$^2$*day (Shillings et.al. 2004:17), $A_{Panels}$ [m$^2$] is the total absorber area of the factory's plant, $\eta_{Solar\ plant}$ [-] is the measured system efficiency of the factory's plant.

### 5.3.5 Thermal Efficiency of Boiler

The thermal efficiency of a boiler is calculated with equation 5.18.

$$\eta_{boiler} = \frac{E_{useful}}{E_{input}} \quad [-] \qquad \text{Eq 5.18}$$

where $E_{useful}$ [kWh] is the thermal energy supplied by the boiler and $E_{input}$ [kWh] is the fuel energy input during the same period.

### 5.3.6 Heat Energy Meter

An ultrasonic heat meter transmits ultrasonic waves between two transducers, through the pipe and fluid of interest in order to calculate its velocity. By attaching temperature sensors to the return and supply pipes of the sink/source the thermal power can be calculated according to equation 5.10.

The transducers, seen mounted on a pipe in figure 5.1, operate both as transmitters and receivers. The ultrasonic waves' transit time between the transducers determine the flow velocity.


**Figure 5.1: Flow transducers mounted on a pipe (Dynameters 2012:7)**

## 5.4 Cooling

The coefficient of performance (COP) for a cooling unit is defined as the relation between the transferred heat and the electricity used by the compressor, according to equation 5.19 (Alvarez 2006:746)

$$COP = \frac{P_{heat}}{P_{el}} \quad [-] \qquad \text{Eq 5.19}$$

$P_{heat}$ [W] is the transferred heat from the cooled facility and $P_{el}$ [W] is the electric power need of the compressor.

## 5.5 Fuels

The higher heating values (HHV) and the cost of fuels (Blaser 2013) are shown in table 5.1. The higher heating value, also denoted gross heating value or gross combustion value, includes the latent heat of vaporization of water in the fuel (Alvarez 2006:500). When considering manufacturers' efficiency statements it is important to note which heating value that is used, the higher or the lower. For the efficiency calculations in this project HHV is used since it seems most reasonable to consider the whole energy content of the fuel. In practice the energy content of fuels differ and the HHV used for diesel and kerosene are averages of 26 sources (Staffell 2011:2). The price of electricity from ECG during the project was 0.47 GHC (Blaser 2013).

A possible source of energy for the factory is waste from the processing of coconuts. The waste consists of shells and some meat (Blaser 2013) but noted in table 5.1 is the value for shells, the part with the lower HHV of the two (Banzon 1980:2). The lower value is used in order to not overestimate the potential of the waste.

Since methane is a single molecule the HHV is always the same, but the methane content of biogas is location-specific. The biogas produced at the factory contains around 52 $_{vol}$% (HPW 2013) of methane, determining the HHV. The stated values for methane and biogas in table 5.1 hold for 25 °C and 1 atm pressure (Ragland and Bryden 2011:13,180).

**Table 5.1: Properties of fuels**

| Fuel | HHV [MJ/kg] | Density [kg/liter] | HHV [kWh/liter] | Cost [GHC/liter] |
|---|---|---|---|---|
| **Diesel** | 45.6 | 0.837 | 10.6 | 2.2 |
| **Kerosene** | 46.0 | 0.807 | 10.3 | 2.0 |
| **Methane** | 55.5 | $0.654*10^{-3}$ | $10.1*10^{-3}$ | - |
| **Biogas (52 % $CH_4$)** | - | - | $5.3*10^{-3}$ | 0 |
| **Coconut waste** | 22.8 | - | - | 0 |

From fuel consumption, the energy return on investment (EROI) can be calculated with equation 5.20.

$$EROI = \frac{E_{produced}}{E_{used}} \quad [-] \qquad \text{Eq 5.20}$$

where $E_{produced}$ [kWh] is the produced amount of energy (energy return) and $E_{used}$ [kWh] is the used (invested) amount of energy.

## 5.6 Cost Calculations

In this chapter theory related to possible reductions of energy costs is presented. The implementations are discussed in chapter 8.

### 5.6.1 Payback Time New Boiler

The payback time for the purchase of a new boiler with improved efficiency is calculated with equation 5.21. In equation 5.21 the investment cost of the new boiler is divided by the daily cost reduction due to improved boiler efficiency.

$$Payback\ time = \frac{C_{boiler}}{\frac{E_{required}}{C_{fuel}} * (\frac{1}{\eta_{old}} - \frac{1}{\eta_{new}})} \qquad \text{[days]} \qquad \text{Eq 5.21}$$

where $C_{fuel}$ [Ghana Cedi, GHC/kWh] is the cost of fuel, $E_{required}$ [kWh/day] is the required energy production from the boiler per day, $\eta$ is the efficiency of the boiler and $C_{boiler}$ [GHC] is the cost of a new boiler.

### 5.6.2 Profit of Using the New Boiler Instead of Biogas CHP

The new boiler mentioned in chapter 5.6.1 can combust both biogas and kerosene. The profit of combusting biogas in the boiler instead of in the biogas CHP is calculated with equation 5.22. The profit is dependent on the higher thermal efficiency of the boiler and the loss of electricity production from the CHP. The loss of electricity is assumed to be replaced by production from the diesel generator. The first term of equation 5.22 describes the decreased kerosene cost due to the difference in thermal efficiency between the boiler and the CHP. The second term describes the increased diesel cost due to the replacement of electricity generation.

$$Profit = E_{gas}\left[\left(1 - \frac{\eta_{th\ CHP}}{\eta_{th\ boiler}}\right) * \frac{C_{ker}}{HHV_{ker}}\right] - E_{gas}\left[\frac{\eta_{el\ CHP}}{\eta_{el\ diesel}} * \frac{C_{diesel}}{HHV_{diesel}}\right] \qquad \text{[GHC]} \qquad \text{Eq 5.22}$$

where $E_{gas}$ [kWh] is the energy content of the daily produced biogas, $\eta_{th\ CHP}/\eta_{th\ boiler}$ are the thermal efficiencies of the biogas CHP and the boiler, $\eta_{el\ CHP}/\eta_{el\ diesel}$ are the electrical efficiencies of the biogas CHP and the diesel generator, $HHV_{ker}/HHV_{diesel}$ [kWh/liter] are the higher heating values of kerosene and diesel, and $C_{ker}/C_{diesel}$ [GHC] are the costs of kerosene and diesel.

### 5.6.3 Payback Time Roaster Boiler

The payback time for the purchase of a new roaster boiler for coconut shells is calculated with equation 5.23. In equation 5.23 the investment cost of the coconut boiler is divided by the daily cost reduction due to less use of kerosene.

$$Payback\ time = \frac{C_{coc\ boiler}}{\frac{E_{coc} * \eta_{coc\ boiler}}{\eta_{ker\ boiler}} * \frac{C_{ker}}{HHV_{ker}}} \qquad \text{[days]} \qquad \text{Eq 5.23}$$

where $C_{coc\ boiler}$ [GHC] is the cost of the coconut boiler, $E_{coc}$ [kWh] is the energy content of the daily coconut waste, $\eta_{coc\ boiler}/\eta_{ker\ boiler}$ are the efficiencies of the coconut boiler and the present kerosene boiler, $C_{ker}$ [GHC] is the cost of kerosene per liter and $HHV_{ker}$ [kWh/liter] is the higher heating value of kerosene.

### 5.6.4 Payback Time Insulation of Solar Plant

The payback time for insulation of the solar plant is calculated with equation 5.24. In equation 5.24 the investment cost of insulation is divided by the daily cost reduction due the increased heat production of the solar plant. The heat is assumed to replace production from the kerosene boiler.

$$Payback\ time = \frac{C_{insulation} * L_{pipe}}{(P_{saved} * T_{sun}) \frac{C_{kerosene}}{\eta_{kerosene} * HHV_{kerosene}}} \quad \text{[days]} \qquad \text{Eq 5.24}$$

where $C_{insulation}$ [GHC/m] is the insulation cost including mineral wool and aluminum sheet (22 GHC/m), $L_{pipe}$ [m] is the total pipe length, $P_{saved}$ [kW] is 50 % of the measured thermal power loss (assuming that the heat losses can be reduced by 50 % when insulating), $T_{sun}$ [h/day] is the number of sun hours per day, $C_{kerosene}$ [GHC] is the cost of kerosene per liter, $\eta_{kerosene}$ is the efficiency of the kerosene boiler and $HHV_{kerosene}$ [kWh/liter] is the higher heating value of kerosene.

### 5.6.5 Payback Time PV Solar Plant

The payback time for the investment in a photovoltaic (PV) solar plant is calculated with equation 5.25. In equation 5.25 the investment cost of the PV plant is divided by the yearly cost reduction due to less purchased or generated electricity.

$$Payback\ time = \frac{P_{W_p} * C_{investment}}{E_{produced} * C_{opportunity}} \quad \text{[years]} \qquad \text{Eq 5.25}$$

where $P_{W_p}$ [kW] is the installed capacity, $C_{investment}$ [GHC/kW$_p$] is the investment cost for the purchase and installation of the complete plant, with inverters and transports included, $E_{produced}$ [kWh] is the electricity produced by the plant during one year and $C_{opportunity}$ [GHC/kWh] is the opportunity cost for the electricity production. $W_p$ is the peak power delivered at STC.

During 2012 the factory received estimates from a manufacturer of installation cost and production of a 240 $m^2$, 30.24 $kW_p$ PV plant installed on the roof of the factory. The approximate investment cost was 4.2 GHC/$W_p$ and the yearly production 40 MWh. (Blaser 2013)

# 6 Method and Execution

## 6.1 Measurements

### 6.1.1 Instruments

For the electricity measurements a multimeter with a current clamp was used (Uni-Trend UT232, figure 6.1). Through measurements of active power the meter calculates the energy consumption/production. Screenshots can be stored onto an internal memory.

For the heat measurements a DMTFB Transit Time Ultrasonic Heat Meter with clamp-on transducers was used (figure 6.1). Flow, velocity, power and temperatures can be logged onto an internal memory card and transferred to a USB flash drive for data analysis.

**Figure 6.1: Multimeter with current clamp and ultrasonic heat energy meter with flow transducers**

### 6.1.2 Main Electrical Loads

The average electric power need of each main load was determined through a 24 hour measurement of energy consumption. Since some of the loads are unsymmetrical, the meter was shifted between the phases every 30$^{th}$ minute during daytime. During the night only the average power of phase 1 was measured and the load distribution between the phases was assumed to be the same as during daytime.

### 6.1.3 Dryers

The average electric power needs for the dryers during runtime were determined through 24 hour measurements of energy consumption. Only one phase was measured since all motors are three phase. Dryer 1-3 could only be measured together. Their on-times during the 24 hours were retrieved from the dryers' monitoring computer. Since the circulation pumps for dryer 1-3 are not connected to the dryers' main board they had to be measured separately. Dryer 4 could be measured alone and without need for a separate pump measurement.

The heat consumption of dryer 4 was measured during two drying cycles of approximately 24 hours each. One cycle started with the dryer cold and the other with the dryer preheated. The average power calculated is based on both cycles. The heat consumption of dryer 3 was also measured throughout two cycles (approximately 20 hours each), but the power calculations are only based on one of them since the other was not representative.

The temperature sensors and flow transducers were mounted outside the shunted circuits of the dryers, since the temperature sensors are too slow to handle the rapid changes of temperature that occurs inside the circuit.

Since some of the fruit processed during one cycle was re-dried on another occasion it was difficult to measure the energy consumption from fresh to fully dry fruit. Instead the amount of water evaporated during the measured cycles was considered. This data was retrieved from the activity log of the production. Only pineapple was dried during the dryer measurements.

The heat recovery of dryer 1 and 4 was measured during one drying cycle. The average power of the recovered heat was calculated as a share of the heat energy input.

### 6.1.4 Cooling System

The average power need during operation for each three phase cooling machine was measured during parts of a day. The Bitzer tandem 2*7.8 A was also measured during the night since it supplies both facilities with and without nighttime operation. The average power needs during operation for the single phase cooling machines were retrieved through one hour measurements of each unit. During the time of measurement only one of the 2*LG 12.5 A for the general office was working.

The assumed running hours per day, as follows, were estimated from interviews and measurements:

- Bitzer tandem 2*7.8 A: 24 h (8 hours daytime, 16 hours nighttime)
- Bitzer tandem 2*10.8 A: 11 h
- Bitzer 2*24.6 A (water cooled): 11 hours
- LG 12.5 A and 6.3 A: 11 hours

For the water cooled machine the additional test described in chapter 6.1.7 was carried out to give the COP.

### 6.1.5 Generators

The efficiency of the diesel generator was determined by measuring the production of electricity and consumption of fuel simultaneously. The quantity of used fuel was determined with the help of a graded bucket. During the three hours of measurement the meter was moved between the phases every 30th minute.

The heat and electricity production of the biogas CHP were measured during five hours of normal electrical load, with Overhead line and New factory connected (see figure 4.1. In addition the electricity production was measured during 15 minutes of heavier loading, with Overhead line and Dryers connected. The consumed gas was noted simultaneously in order to calculate the thermal and electrical efficiency.

Since the biogas CHP is the only production unit utilizing the biogas at the moment, the amount of gas used by the motor is equal to the total amount produced by the biogas plant. The instantaneous and total amount of produced gas can be retrieved from a gas flow meter, and the technical staff records the daily production.

The daily heat production of the biogas CHP was estimated from the heat and electricity measurements described above, together with the daily recordings of electricity production noted by the technical staff. To calculate the daily heat production, the ratio between the produced heat and electricity from the measurements was multiplied with the daily recordings of electricity production.

### 6.1.6 Kerosene Boiler

The heat production of the kerosene boiler was measured on two occasions, the first during 24 hours, and the second during eight days (8*24 hours). The kerosene consumed was recorded simultaneously by the technical staff, which enabled a calculation of the boiler's thermal efficiency. The temperature sensors and flow transducers were mounted outside of the boiler's shunted circuit.

### 6.1.7 Biogas Plant

The average electric power need during operation for each motor in table 4.2 was measured at least once. The daily runtimes for the motors were estimated from interviews and measurements. The same pump is used for shred waste and feeding of fermenters. The assumed running hours per day are:

- Shredder and pump for shred waste: 4 hours each
- Stirrers: 2 hours each
- Mixer: 7 hours
- Pump for feeding: 3 hours

The heat consumption of the biogas plant was assumed to be equivalent to the heat removed from the water cooled cooling machine. The heat production and electricity consumption of the Bitzer 2*24.6 A were measured simultaneously during seven hours. The temperature sensors were mounted on the supply and return of the heat exchanger but due to air in the piping system the flow meter was malfunctioning. Instead the two analogue (not digital) flow meters installed on the fermenters were used. From that the average power supplied to the biogas plant could be calculated.

For calculation of the biogas plant's EROI the diesel consumption of the tractors was disregarded. The tractors are used for pumping and transportation of effluent from the fermentation tanks to the factory's pineapple fields.

### 6.1.8 Solar Plant

The heat production of the solar plant was measured during seven hours of sunshine. The equipment was mounted on the supply and return pipe of the west side panels. Since the temperature sensors react slower than the flow transducers, the instantaneous thermal power calculations become inaccurate when measuring systems with rapid temperature changes, as the case with the solar plant. Therefore, when processing the data, only periods of steady state were considered.

### 6.1.9 Heat Losses Pipings

The heat losses from pipings were measured by mounting the two temperature sensors on the same pipe with a distance of 18 meters in between. The temperature drop between the sensors corresponds to a power loss. The flow transducers were mounted on the same pipe as the temperature sensors. The same measurement was performed with and without insulation to show the differences in power loss. The supply pipe to dryer 2 was used for both measurements.

The actual heat losses were not possible to retrieve since the offsets of the temperature sensors were larger than the actual temperature difference. Therefore only the *difference* in power loss between the insulated and uninsulated pipe was calculated. However, the main reason to measure the power loss was to quantify the reduction of energy consumption from insulating the piping.

To verify that the measurement result was in the right range a theoretical power loss from an uninsulated pipe was calculated according to chapter 5.3.3.

The ratio between the measured and theoretical power loss at 70 °C was assumed to hold also for 65 °C and 85 °C. The assumption was used to calculate the power losses at these temperatures.

## 6.2 Data Analysis

Data from the heat energy meter is stored in csv-files and was processed and analyzed in Excel. In most cases the static error of the flow meter was zeroed before the measurement was started, but when that was not possible it had to be removed from the logged data.

The analysis of the data from electricity measurements was performed in Excel.

## 6.3 Drawings

The drawing of the electricity system was created with Scheme-it, an online software produced by Digi-Key Corporation.

## 6.4 Trainings

The factory’s technical staff was trained through a common discussion about possible reasons, consequences and solutions to the problems discovered during the project. Furthermore, workshops on heat and electricity measurements and analysis were held. In addition quick start guides and an instruction video for the meters were created. During the workshops the staff had the opportunity to learn more about the theory behind flows of heat and electricity.

# 7 Results

## 7.1 Main Electrical Loads

The factory's total consumption of electricity during the time of measurement was 1700 kWh per day. The average powers of the main loads are presented in table 7.1 and in figure 7.1. The maximum power is the largest average power measured during a 30 minutes period. When comparing figure 7.1 and 7.5, remember that the circulation pumps for dryer 1-3 are connected to the load Old factory. That gives the difference between the *load* Dryers in figure 7.1 and the *user* Dryers in figure 7.5.

**Table 7.1: Average power of the main loads**

| Load | Power 24 hours [kW] | Power daytime [kW] | Power nighttime [kW] | Power maximum [kW] |
|---|---|---|---|---|
| **Old factory** | 18 | 24 | 13 | 29 |
| **Dryers** | 35 | 31 | 36 | 43 |
| **New factory** | 13 | 24 | 7.2 | 30 |
| **Overhead line** | 6.0 | 7.3 | 5.4 | 13 |
| **Total** | **71** | **87** | **61** | **114** |

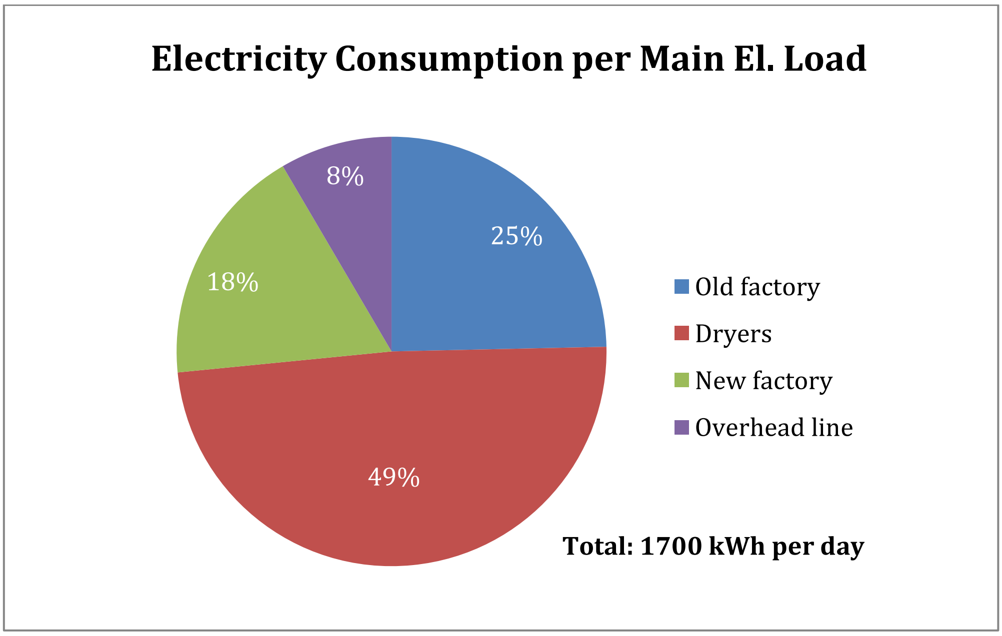


**Figure 7.1: Electricity consumption of the main loads**

The load distribution between the phases of the main loads can be seen in table 7.2, where the power is normalized with respect to phase 1. The table shows the balance between the phases. Note that the loads Old factory and Overhead line are considerably unbalanced.

Table 7.2: Load balance of the main loads

| Load | Power phase 1 | Power phase 2 | Power phase 3 |
|---|---|---|---|
| **Old factory** | 1 | 1.6 | 0.6 |
| **Dryers** | 1 | 1 | 1.1 |
| **New factory** | 1 | 0.93 | 1 |
| **Overhead line** | 1 | 0.86 | 1.6 |
| **Total** | 1 | 1.1 | 0.95 |

## 7.2 Dryers

The factory's daily production of heat for the fruit dryers was 7200 kWh during the time of measurement. Figure 7.2 shows the heat production per production unit, with results from chapter 7.4, 7.5, 7.6 and 7.7. The production can be compared to the heat consumption of the dryers. The average thermal power was 75 $kW_{th}$ for dryer 1-3, and 186 $kW_{th}$ for dryer 4, implied by the thermal power plots in figure 7.3 and 7.4. With an assumption of 18 hours runtime per dryer and day the heat consumption would be 7400 kWh. The measurements of heat production and consumption were not performed simultaneously and only during a limited time, hence the comparison should be considered to be approximate.

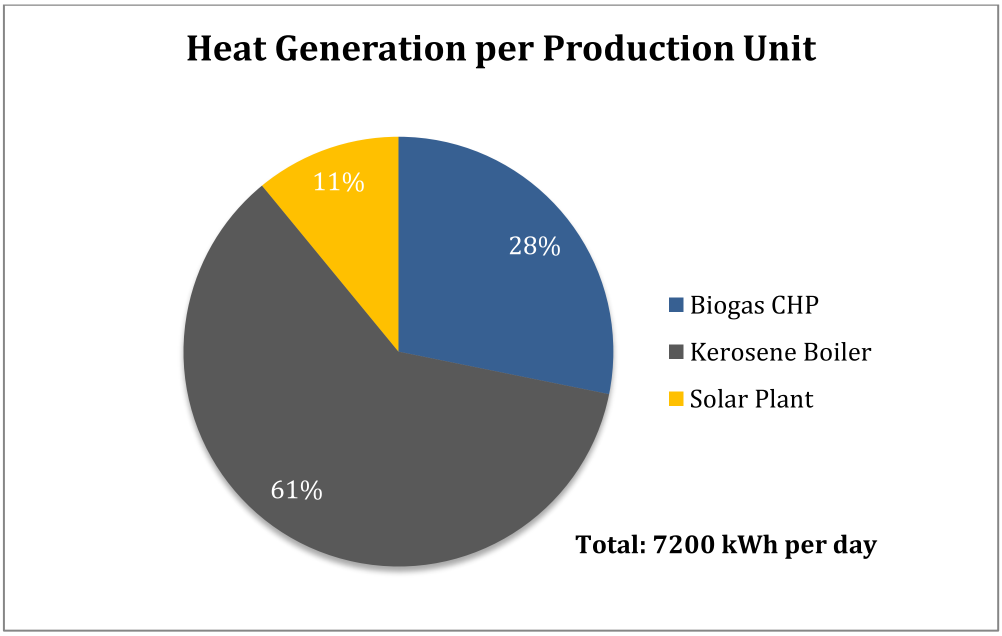


Figure 7.2: Heat generation for dryers, per production unit

Table 7.3 presents the results from the measurements of the dryers, where the consumed energy is given per kilogram of evaporated water. The flow rate and the temperature difference are given for when the shunt is fully open, while the other values are averages over the measured cycles. The thermal power needs of dryer 3 and 4, measured during one cycle, can be seen in figure 7.3 and 7.4.

**Table 7.3: Results from measurements of the dryers**

| Dryer | Flow rate [$m^3/h$] | Temp diff [°C] | Heat consumption [$kWh/kg_{water}$] | Heat recovery [%] | Electrical power [kW] | Electricity consumption [$kWh/kg_{water}$] |
|---|---|---|---|---|---|---|
| **Dryer 4** | 16 | 15 | 0.64 | 8.7 | 17 | 0.063 |
| **Dryer 3** | 8.7 | 12 | 0.57 | 6.1 | 11 | 0.083 |

Figure 7.3 and 7.4 illustrate that the dryers need maximum thermal power during half of the drying program. The high power is needed to sustain the temperature and humidity set points during a period of large evaporation.

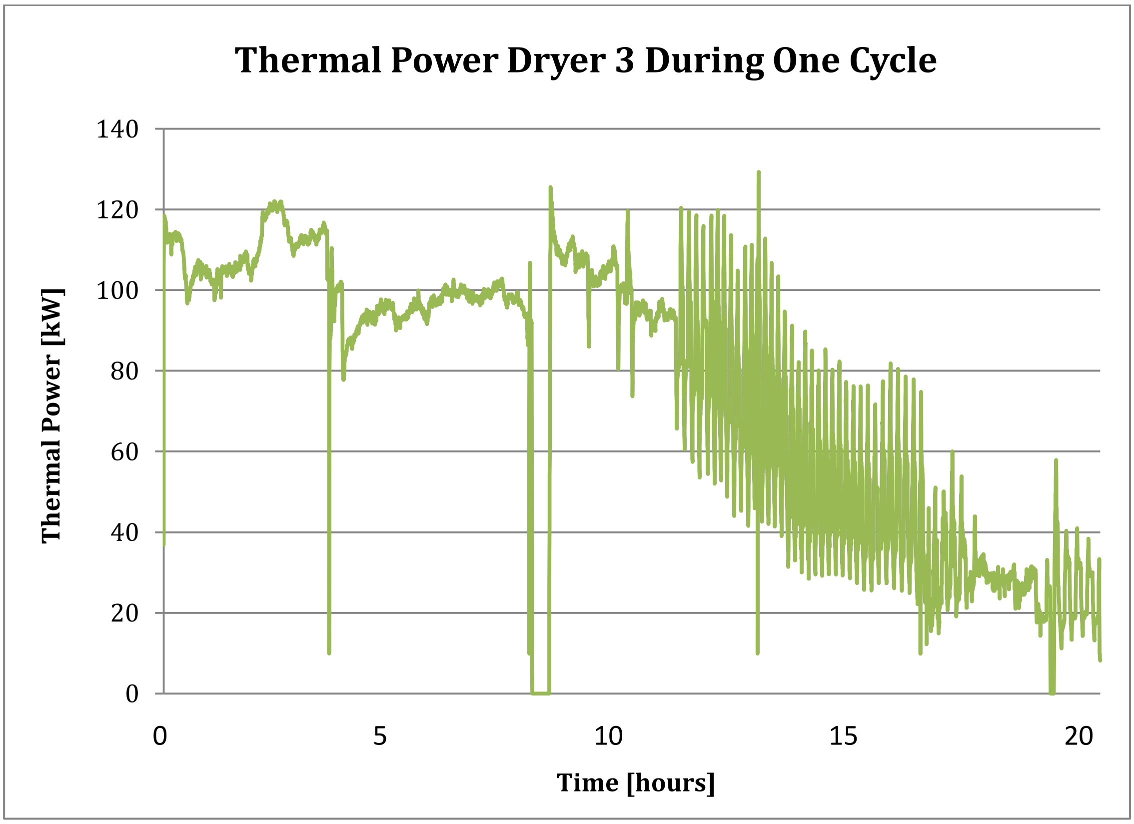


**Figure 7.3: Thermal power of dryer 3 during one cycle**

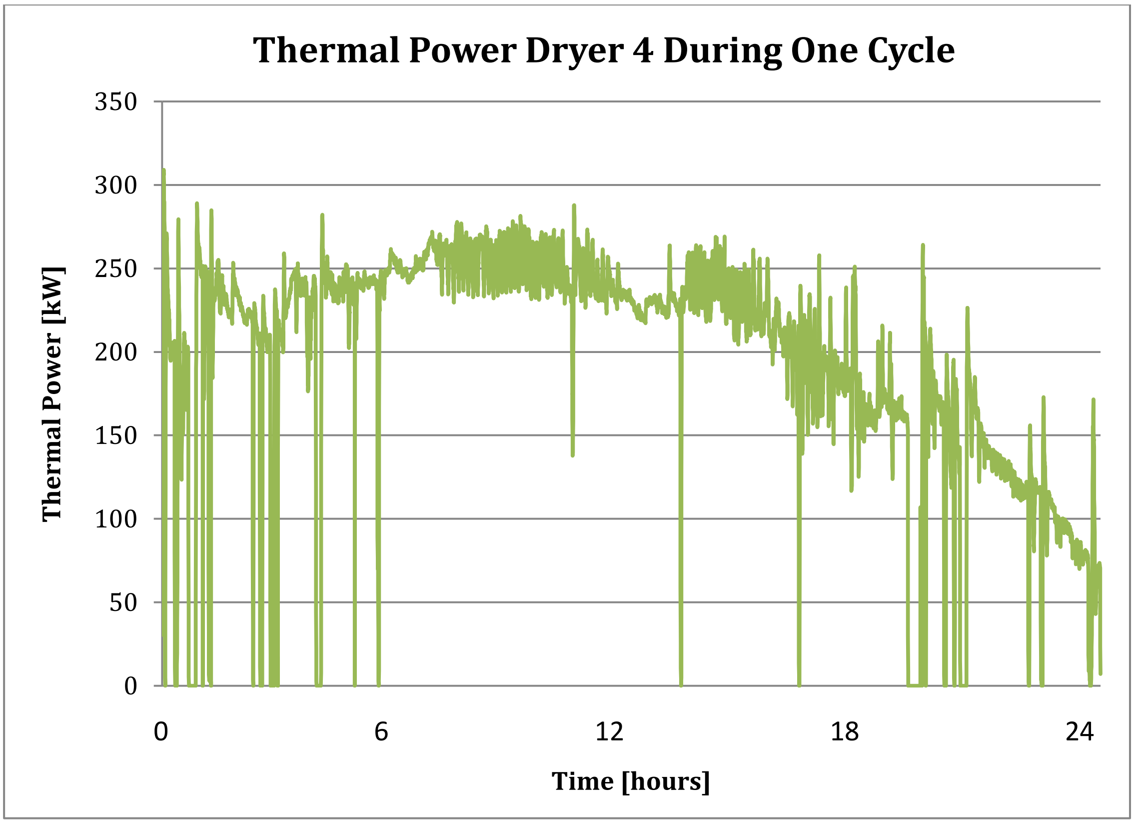


**Figure 7.4: Thermal power of dryer 4 during one cycle**

The electricity consumption of the fruit dryers varies from day to day since the fruit production differs. The measurements of the main loads indicate a consumption of 860 kWh per day for all four dryers, with the circulation pumps for dryer 1-3 included. In other words roughly half of the consumed electricity goes to the dryers, which is illustrated by figure 7.5. Figure 7.5 includes results from chapter 7.1, 7.3 and 7.6.

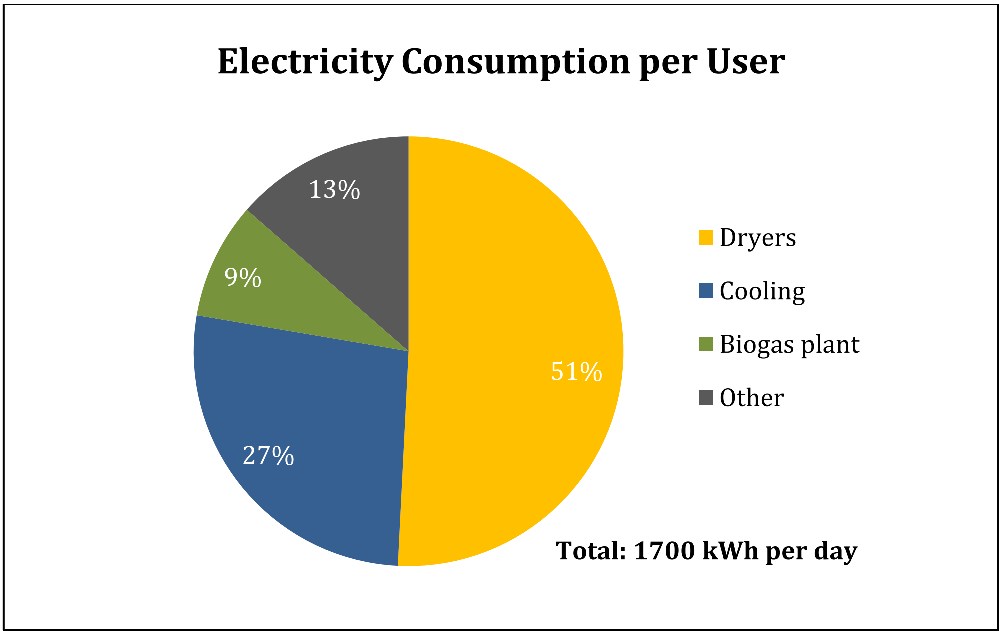


**Figure 7.5: The factory's electricity consumption per user**

## 7.3 Cooling system

The electricity consumption of the cooling machines is shown in table 7.4. The complete system consumes 450 kWh per day, corresponding to 27 % of the factory's total electricity consumption.

**Table 7.4: Electricity consumption of the factory's cooling machines**

| Cooling unit | Power day [kW] | Power night [kW] | Daily consumption [kWh] |
|---|---|---|---|
| **Bitzer tandem 2*7.8 A** | 6.2 | 2.9 | 96 |
| **Bitzer tandem 2*10.8 A** | 3.6 | - | 39 |
| **Bitzer 2*24.6 A** | 13 | - | 143 |
| **Bitzer 1*15.9 A** | 4.6 | 4.6 | 110 |
| **LG 12.5 A + LG 6.3 A** | 2.9 | - | 32 |
| **LG 12.5 A** | 0.6 | - | 6,6 |
| **2*LG 12.5 A** | 2.2 | - | 24 |
| **Total** | 33 | 7.5 | 450 |

Table 7.4 and 4.1 show that there are excess cooling capacity for both Bitzer tandem 2*10.8 A and Bitzer 2*24.6 A.

The results from testing the water cooled Bitzer 2*24.6 A are shown in table 7.5. The supply and return temperatures, water flow and heat removed relate to the water cooled circuit connected to the condenser and biogas plant. The COP is calculated with equation 5.19.

**Table 7.5: Results from the additional test of Bitzer 2*24.6 A**

| Cooling machine | Supply temp [°C] | Return temp [°C] | Water flow [$m^3/h$] | Heat removed [kW] | El power need [kW] | COP [-] |
|---|---|---|---|---|---|---|
| **Bitzer 2*24.6 A** | 50 | 41 | 3.4 | 36 | 13 | 2.8 |

## 7.4 Generators

Results from performance tests of the diesel generator and the biogas CHP can be seen in table 7.6 (efficiencies calculated with equation 5.18). Note that 55 % of the energy input to the biogas CHP converts to heat losses, and that the electrical efficiency increased by 33 % when the generator was loaded close to its practical upper limit. The electrical efficiency of 9 % during normal running conditions has been verified from recordings of production and consumption over a longer time period. The maximum current measured for the diesel generator through the heaviest loaded phase was around 140 A.

Table 7.6: Results from measurements of the generators

| Generator | El power [kW] | El eff [%] | Thermal power [kW] | Thermal eff [%] |
|---|---|---|---|---|
| **Diesel gen** | 72 | 29 | - | - |
| **Biogas CHP** | 27 | 8.6 | 113 | 36 |
| **Biogas CHP** | 43 | 12 | - | - |

Figure 7.6 shows the return temperature from the storage tank to the biogas CHP during 5.5 hours of measurement. The plot illustrates a problem that repeatedly occurs in the heat system - the return temperature from the storage tank increases above the return temperature from the dryers. This phenomenon was noted also when measuring the solar plant. The reason is that the storage tank is dimensioned only for the solar plant and dryer 1-3 (Blaser 2013). Since the solar plant was installed more units have been connected to the tank (dryer 4, the kerosene boiler and the CHP-generators), frequently causing overloading with consecutive reshuffling and loss of adequate stratification.

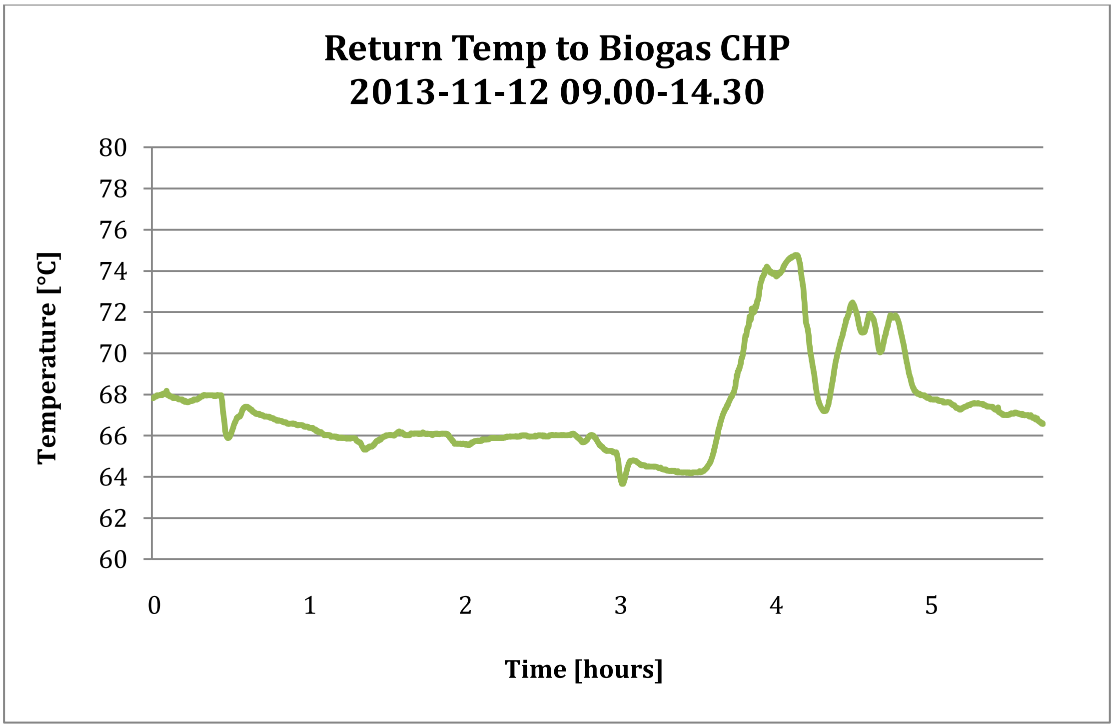


**Figure 7.6: Temperature of the return from the storage tank to the biogas CHP during 5.5 hours**

## 7.5 Kerosene Boiler

The thermal efficiency of the kerosene boiler, calculated with equation 5.18, was 73 % during the shorter measurement of 24 hours, and 69 % during the longer measurement period of eight days (8*24 hours). The average thermal power was 320 kW during operation. The per-day consumption of fuel was 620 liters, corresponding to 6370 kWh. That means the actual heat production from the kerosene boiler, with 69 % efficiency, was 4400 kWh per day.

## 7.6 Biogas Plant

Table 7.7 shows the biogas plant's per-day consumption of electricity and heat together with the biogas produced in terms of energy. As illustrated by figure 7.5 the biogas plant's share of the factory's total electricity consumption is 9 %. When considering the energy content of the produced biogas the EROI is 11. When the biogas is converted to heat and electricity by the biogas CHP the EROI decreases to 5.1 (3.6 for electricity and 5.6 for heat).

**Table 7.7: The biogas plant's consumption of electricity and heat**

| Unit | Heat consump [kWh] | El consump [kWh] | Biogas prod [kWh] | EROI |
|---|---|---|---|---|
| **Biogas plant** | 380 | 70 | 5650 | 11 |

The measured power needs for the motors connected to the biogas plant are presented in table 7.8.

**Table 7.8: Power needs for motors connected to the biogas plant**

| Motor | Power need [kW] |
|---|---|
| **Shredder** | 4.4 |
| **Pump for shred waste** | 8.3 |
| **Pump for feeding** | 9.0 |
| **Mixer** | 4.6 |
| **Stirrer** | 9.3 |

## 7.7 Heat Losses Pipings

The measured difference in heat loss between insulated and uninsulated pipes at 70 °C was 140 W/m. The theoretical power loss from an uninsulated 2 inch steel pipe was calculated to 85 W/m (equations in chapter 5.3.3).

The thermal power loss per meter pipe at 85 °C and 65 °C was calculated to 210 W and 120 W (method chapter 6.1.9). These results are used for the solar plant heat loss calculations in chapter 7.8.

## 7.8 Solar Plant

During the time of measurement the average power delivered by the west side of the solar plant was 80 kW when the sun was shining and the circulation pumps were running. The average supply and return temperatures were 85 °C and 65 °C. The flow was 3.5-3.9 $m^3$/h when the pumps were on.

With a thermal power of 80 kW the system efficiency of the west solar plant was calculated to 29 % (equation 5.11). The solar plant uses 140 meters of supply pipes and 118 meters of return pipes equally divided between the two sides. Due to lack of insulation this causes an approximate thermal power loss (for the complete plant) of

42 kW when the circulation pumps are running (results from 7.7). With the heat losses from pipings of the west side (21 kW) subtracted the panel efficiency is 36 %. If equal efficiency is assumed for the panels on the east side the daily energy production of the complete solar plant is around 800 kWh (equation 5.17).

Figure 7.7 shows the supply and return temperature of the solar plant during a limited period of the measurement, illustrating the problem with overloading of the heat storage tank. Note that the tank bottom temperature is 80 °C, i.e. equal to the required supply temperature for the dryers. That gives a solar plant supply temperature close to 100 °C.

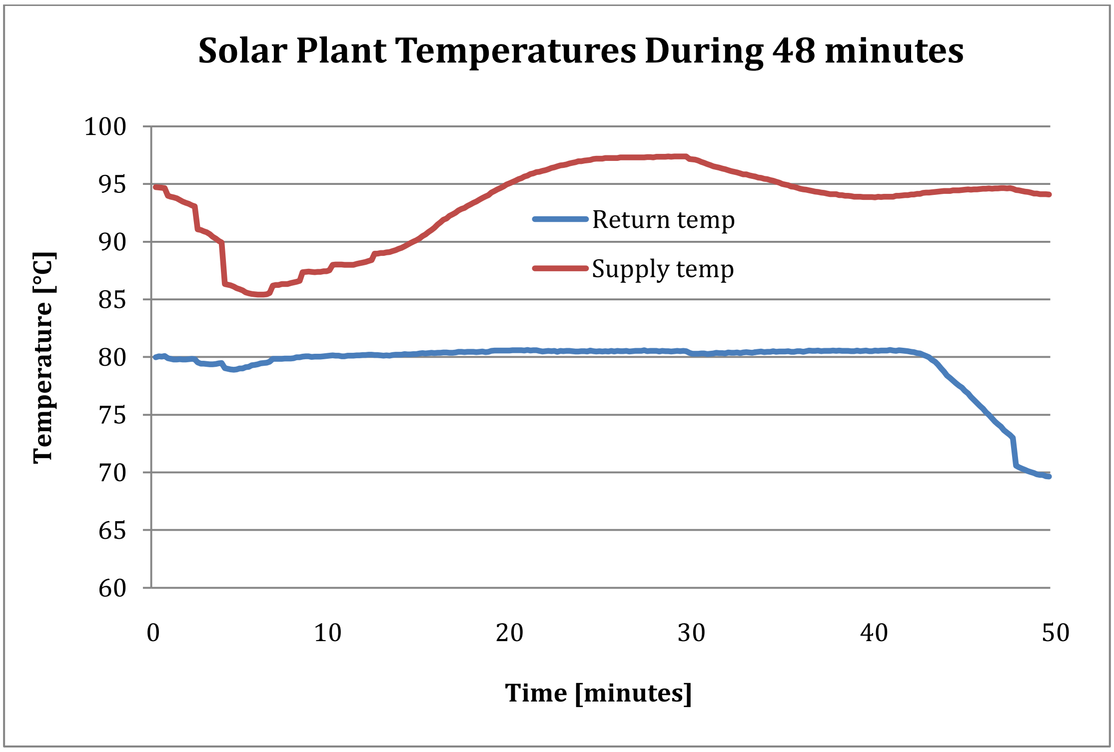


**Figure 7.7: Power needs for motors connected to the biogas plant**

## 7.9 Trainings

Quick start guides for the meters and pictures from the workshops can be found in appendix 1-3.

# 8 Conclusions and Discussion

## 8.1 Sources of Errors

The project results should be read with several possible sources of errors in mind. Furthermore, the results should not be seen as valid for the whole year since the fruit and climate change with the seasons. The dryers consume less heat when the intake air is hot and dry. The cooling system consumes less electricity when the air is cold and wet. The project has been carried out between the (cold and wet) rainy season and the (hot and dry) harmattan season. Hence the results might be considered as rough averages of yearly values.

For the calculations of profit and payback time, restrictive numbers and assumptions have been used in an attempt to not exaggerate the benefits of the measures.

### 8.1.1 Meters

The temperature sensors of the heat meter have a stated accuracy of 0.1 °C (Dynameters 2012:49) but it looks as if they have static errors. A possible static error would affect measurements with small temperature differences, e.g. the heat recovery of the dryers. The errors should have been zeroed during the factory calibration but the calibration data sheet says nothing about calibration of temperature sensors. The stated accuracy of the flow transducers is 1 % (Dynameters 2012:3) but a perfect mounting is not achievable. Furthermore, the wall thickness and diameters of the pipes are varying because of manufacturing tolerances and deposits in pipes.

The electricity meter has a stated accuracy of 3 % for the power measurements (PCE Group 2013:26). The mounting of the meter should not cause any significant error.

The gas flow meter has a stated accuracy of 0.5 % (ABB 2011:106).

### 8.1.2 Runtime Assumptions

The assumed runtimes of the measured units are based on recordings from the technical staff, the monitoring computer, interviews and observations. The actual runtimes will always differ from the assumed, but to what extent is difficult to tell.

### 8.1.3 Recordings of Processed Fruit

For the dryer measurements the greatest source of error is probably the readings of fresh and dry fruit weight from the activity log, since it was difficult to retrieve the exact quantities during the particular time of measurement.

### 8.1.4 Measurement of Diesel Generator

The accuracy of the graded bucket used for the measurement of the diesel generator is most likely low. Furthermore, to discharge the bucket without spilling was practically impossible.

## 8.2 Main Electrical Loads

The insufficient balance of the main loads Old factory and Overhead line (table 7.2) is probably caused by single phase machines connected without consideration of balance. Overhead line feeds six single phase 1.2 kW pumps for the boreholes. Old factory feeds two single phase 3 kW pumps (not run simultaneously) as well as all the single phase cooling machines for the old factory. (Blaser 2013)

These machines could easily be shifted between the phases to balance the main loads. The unbalanced loads cause several problems, which are discussed further in chapter 8.5.

## 8.3 Dryers

The dryers do not perform as they should in terms of power output. From figure 7.3 and 7.4 and chapter 4.2 the ratio between the actual maximum thermal power and rated power was calculated to 55 % for dryer 3 and 45 % for dryer 4. The low power output is not necessarily negative in terms of energy efficiency, but in order to dry faster the power output needs to increase. Given that the present temperature difference over the heat exchanger can be kept by increasing the volume of intake air, the rated thermal powers would be reached if the maximum flow increases from 8.7 to 14 $m^3/h$ for dryer 3 and from 16 to 31 $m^3/h$ for dryer 4 (equation 5.10). When the dryers were installed the pipes were dimensioned for flows in this order of magnitude, meaning that installation of new pipes is not necessary.

A system like this, with zero static pressure head, many running hours and large flow variations usually benefits from frequency regulated pumps (Blomström 2013:38). If higher-capacity pumps are installed the shunt would most likely choke the inlet flow during a larger share of the cycle, increasing the advantage of frequency regulated pumps. That has not been investigated further in this project but should be considered before the installation of new pumps.

The heat recoveries of the dryers differ in performance (table 7.3). During measurements the heat recovery of dryer 4 was 9 %, which should be compared to the 11 % stated by the manufacturer (RW De Beer 2012). For dryer 3 the recovery was 6 % compared to the stated 18 % (RW De Beer 2010). The low output from the heat recovery of dryer 3 is probably due to corrosion from sulfur (Blaser 2013). The fresh cut fruit is sprayed with sulfur before it enters the dryers to prevent color changes. When the exhaust gases condense on the aluminum fins of the heat exchangers the sulfur stays on the surface causing corrosion. The heat exchangers of dryer 1-3 are made of aluminum, while dryer 4’s is made of stainless steel that is less sulfur-sensitive. Regardless of material, the heat recovery can be improved by insulating the pipes between inlet and outlet. Furthermore, exhaust gases are leaking from insufficiently sealed outlets and intakes/outlets without louvers. The dryers are namely constructed with only one louver to regulate the intake and exhaust air, giving leakage also when the louver is closed due to convection and pressure difference.

The consumed heat per amount of evaporated water was supposed to show the performance of the dryers. According to the measurements dryer 3 and 4 consumed 0.57 and 0.64 kWh per kilogram evaporated water (table 7.3). The dryer manufacturer states that the heat consumption per kilogram water is around 1 kWh (RW De Beer 2010, 2012). The actual performance is probably not better than that, leading to the assumption that the measurements are not reliable. Uncertainties in the results are discussed in chapter 8.1.3.

Today the majority of the heat delivered to the dryers is produced from the fossil fuel kerosene (figure 7.2). With improved efficiency of the solar plant, a new boiler for biogas and a roaster boiler for coconut shells, discussed in chapter 8.6 and 8.8, the factory could become self-sufficient on heat for the dryers. As seen in figure 8.1 the heat production would be 100 % renewable. The per-day heat production of 7800 kWh should be compared to the present 7200 kWh (chapter 7.2). The assumed efficiencies of the biogas boiler, solar plant and coconut boiler are 90, 50 and 60 % respectively. See chapter 8.6 and 8.8 for further discussions about the production units.

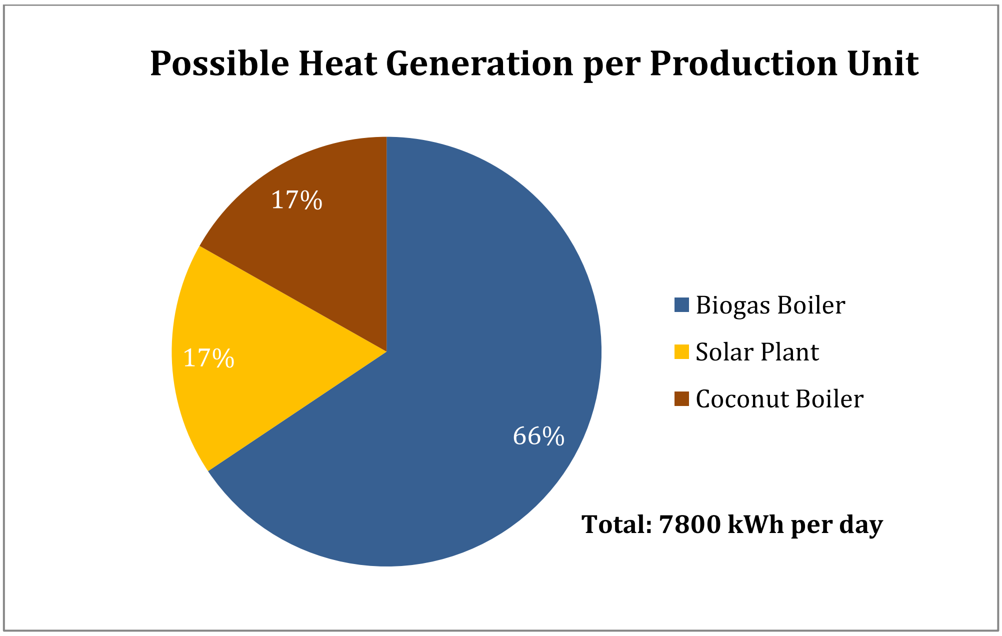


**Figure 8.1: Possible future heat generation for dryers, per production unit**

## 8.4 Cooling System

The cooling system of the factory is a substantial user of electricity but has great improvement potential. The cooling capacity of the evaporators connected to Bitzer tandem 2*10.8 A is around 8 kW less than the compressor's capacity (chapter 4.3). The measurements indicate that the utilization of the machine is far less (table 7.4). The sum of power needs of the single phase machines are 5.7 kW, while the power need for Bitzer tandem 2*10.8 A is 3.6 kW (table 7.4). With the restrictive assumption that the power needs of Bitzer tandem 2*10.8 A and the single phase machines are equal (i.e. equal COP), the excess capacity of Bitzer tandem 2*10.8 A is enough to cool the general office, the lab and the local processing room. By using fewer cooling machines at higher efficiency the electricity consumption and maintenance costs would decrease. The manufacturer's specifications do not contain information about COP for the evaporator and condenser temperatures at the factory.

The measurements show that the utilization of Bitzer 2*24.6 A is also very low (table 7.4). That is partly because one of the compressors is regularly shut off. The reason is that the heat removed from the condenser is not enough in order to run both compressors at the same time (Blaser 2013). The heat flow of the circuit could be increased by lowering the condenser inlet temperature and/or increase the flow. Apart from releasing the full cooling capacity of the machine, the COP and lifespan would increase. One way of reducing the temperature to the condenser is to install an air cooler on the return pipe between the biogas plant and the condenser. However, the cost of higher efficiency for the cooling machine would be the additional need of electricity for pumping and running of fans. Another solution was presented by the factory manager: increase the flow by installing a new pump and connect new uninsulated return pipes from the biogas plant that are cooled by the waste water treatment plant (Blaser 2013).

Furthermore, three LG 12.5 A cooling machines have been installed in a new office that was built during the project. The excess capacity of Bitzer 2*24.6 A would easily be enough to do the work of the three single phase machines. Though, the distance between the cooling machine and the new office might be too far.

If the cooling machines of the general office are not replaced, the condensers should be moved closer to the ceiling to get better protection from the afternoon sun. The current position is depicted in figure 8.2.


**Figure 8.2: Placement of condensers for general office's cooling machines**

The low-exergy heat from the condensers of the cooling machines could be used to preheat the intake air to the dryers. A possible solution is to connect air ducts directly from the condensers to the inlet. To ensure sufficient air flow for the dryers and the condensers at all time, a louver that opens when the dryer inlet is closed or when the cooling machine is off can be installed in the duct.

Finally, to cut the cooling need the thermal losses from cooled facilities could be reduced. A few construction flaws have been noticed:

- The insulation of windows and doors in cooled facilities is insufficient.
- Some windows and doors do not fit or close properly, e.g. the doors to General office and Business development/Quality assurance.
- Some windows of cooled facilities are not shaded with screens, see for example figure 8.2.

The thermal losses should always be considered when renovating or planning for new buildings with cooling. Furthermore, the temperature of cooled facilities should be set as high as possible without interfering with the purpose of the cooling.

## 8.5 Generators

The efficiency of the biogas CHP is poor (9 % electrical, 29 % thermal, table 7.6). This results in daily heat losses of approximately 3100 kWh. A better use of the biogas is discussed in chapter 8.6. At the beginning of the project the power from the ECG was very unstable, with large voltage fluctuations and many blackouts. During blackout the diesel generator and biogas CHP have to be run together in order to cover the complete load. However, the maximum load of the factory is 114 kW (30 minutes average, table 7.1), i.e. less than the rated capacity of one of the generators. One part of the problem is the unbalanced loads (table 7.2) which cause uneven torque throughout the revolution of the rotor. That reduces the power output and efficiency while increasing the wear of bearings.

In addition, the biogas CHP is probably dimensioned and rated for natural gas (Blaser 2013), i.e. a fuel with almost twice the methane content. That would explain why the full load power output is roughly half of the rated. Furthermore, the efficiency of a generator is generally lower at part load (Petchers 2002:503), which was confirmed by the full-load test of the biogas CHP, giving an increased efficiency (table 7.6). Since the biogas boiler is malfunctioning the biogas can only be combusted in the CHP at the moment. Due to the higher efficiency at full load the generator should be synchronized as much as possible to the grid in order to maximize the power output.

The diesel generator is performing according to specifications in terms of fuel consumption. The measured electrical efficiency of 29 % (table 7.6) corresponds to a consumption of 0.33 liter/kWh, and the manufacturer states 0.35 liter/kWh at 50 % load (Olympian 2012:2). However, the maximum possible loading of the generator is not close to the rated. The rated prime power is 150 kVA while the standby power (available for one hour) is 165 kVA (Olympian 2012:1), equivalent to currents of 209 and 230 A. The practical maximum current of the heaviest loaded phase is around 140 A (chapter 7.4). The load rate could be increased slightly by balancing the loads, and the extent of improvement can be determined by loading the generator with load banks. This test should be performed by technicians from CAT, who could also find defects causing the low power output.

During the time of project work a new transformer was installed that reduced the voltage fluctuations, resulting in a greater utilization of the ECG. Still the blackouts are frequent resulting in a need for backup generation that can cover the full load. For that reason the factory is bidding on an old but unused 500 kVA diesel generator. With such a big generator capacity the biogas CHP could be set aside. However, the maximum measured load of the factory was 114 kW (table 7.1), i.e. less than 30 % of 500 kVA (at power factor 0.8). As discussed before, the efficiency of a generator usually decreases when loaded light.

Neither the present nor the possible new diesel generator is equipped with a system for heat recovery. For the 150 kVA generator there is equipment waiting for installation (Blaser 2013). The benefit of buying equipment for the possible 500 kVA generator is uncertain since the utilization of the ECG just recently increased. The future number of running hours of the backup generators will tell if such an investment is advisable.

The same holds for the possible purchase of a new biogas CHP with better efficiency, i.e. the benefit of generating electricity from a biogas CHP is dependent on which generation that is replaced. Because of the mentioned uncertainty this is not investigated further in the project.

## 8.6 Boilers

The measurements showed that the efficiency of the kerosene boiler is poor (69 %, chapter 7.5), partly because of the leaky burner intake depicted in figure 8.3. The factory manager has already ordered a new 620 kW boiler with a stated efficiency of 92 %. If the stated efficiency is correct, the payback time for the new boiler, costing 30 000 GHC, is 104 days (equation 5.21, table 5.1, chapter 7.5).

**Figure 8.3: Leaky burner intake of kerosene boiler**

The new boiler can burn both biogas and kerosene. Instead of running the biogas CHP, the gas could be used in the boiler, increasing the thermal efficiency at the cost of less electricity generation. For the stated efficiency of 92 % the profit of this measure is 304 GHC per day. The calculation assumes that the loss of electricity generation (at normal biogas CHP load) is covered for by the diesel generator, and that the additional heat produced reduces the use of kerosene (used in the new boiler). It does not take into consideration the cut of maintenance costs of the biogas CHP. Figure 8.4 shows the profit of using the biogas in the new boiler for boiler efficiencies from 40 to 90 % (equation 5.22, table 5.1 and 7.6, chapter 7.5).

This measure will also reduce the use of fossil fuels since the consumption of kerosene (for heat generation) decreases more than the consumption of diesel (for electricity generation) increases.

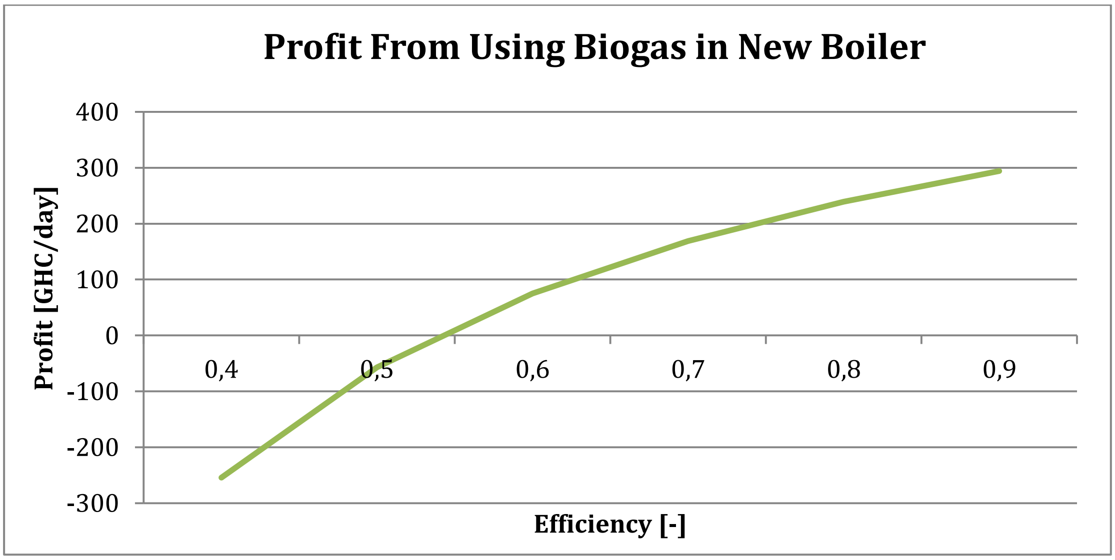


**Figure 8.4: Profit from using biogas in a new boiler instead of in the CHP**

Another possible use of the biogas is to burn it in a direct heated dryer, with less thermal losses. The factory plans to install a new dryer within a year, and the manufacturer provides direct heated dryers (Blaser 2013, RW De Beer 2010).

The factory has started to process coconuts that could give around 120 tons of combustible waste per year (Blaser 2013). The factory manager has got an offer for a 240 kW roaster boiler for solid fuels, costing 42500 GHC (Blaser 2013). The payback time is presented in figure 8.5 for roaster boiler efficiencies from 60 to 90 % (equation 5.23, table 5.1, chapter 7.5). The heat produced by the coconut boiler is assumed to replace heat produced by the present kerosene boiler. A roaster boiler could also be useful for the combustion of other solid waste with acceptable emissions. Furthermore, to combust the shells in a boiler would be a good way of managing the waste.

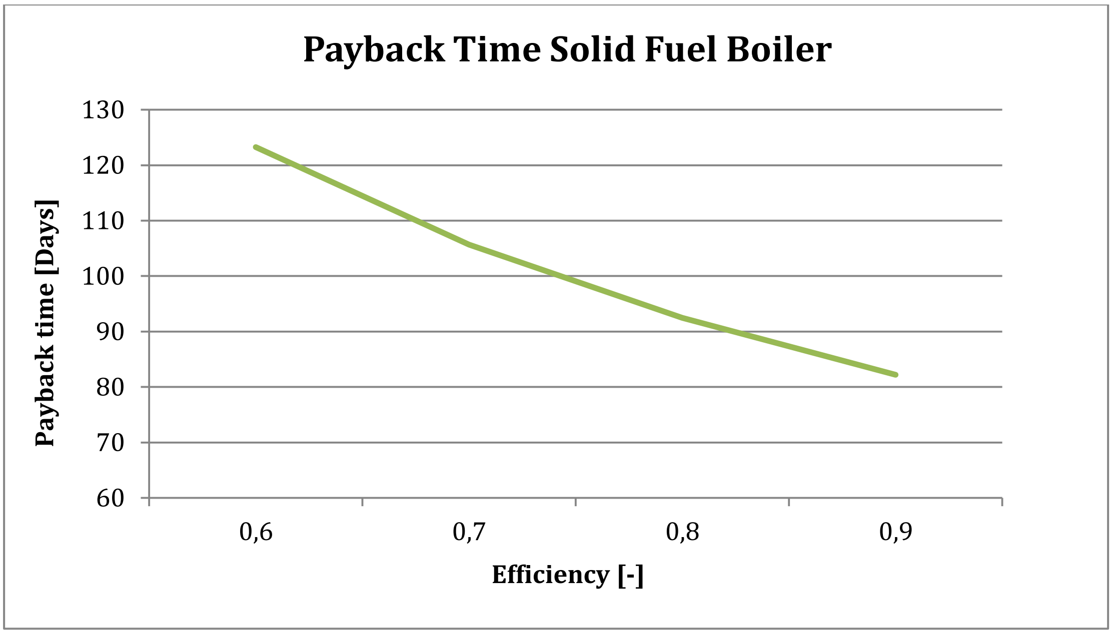


**Figure 8.5: Payback time for the purchase of a roaster boiler for coconut shells**

## 8.7 Biogas Plant

The biogas plant produces large quantities of gas (table 7.7) but 55 % of the energy is converted to heat losses by the biogas CHP (table 7.6). A possible solution to this problem has been discussed in chapter 8.6.

The electricity consumption of the biogas plant could be reduced if the technical staff would be more careful to use the shredder and the pump only when it is needed. The motors are frequently left running even though all of the waste is shredded.

The methane yield of the produced gas is fairly low (52 %, table 5.1). As discussed in chapter 8.5 the low methane content reduces the efficiency of the biogas CHP. Both the methane content and the biogas production would increase if fats were added to the fermentation tanks continuously (Aklaku 2013). However, fats can give foam formation if it is not added cautiously (Sundberg 2014). A suitable source of fats would be the residues of palm oil production. There are several local production units nearby, each producing residues in the range of 50-100 kg/day. The factory has previously attempted to collect the residues but the producers had problems with continuous supply. (Blaser 2013)

## 8.8 Solar Plant

The efficiency of the factory's solar plant is mediocre (29 %, chapter 7.7) but could probably be improved significantly. With an ambient temperature of 30°C and an average absorber temperature of 75°C the rated efficiency of the solar panels is 55 % (Guangdong 2011).

To insulate the pipes would be beneficial. The total investment cost for insulating all piping on the roof would be 3500 GHC (equation 5.24, table 5.1, chapter 5.6.4, 7.5 and 7.7). The payback time is shown in figure 8.6, as a function of the yearly average number of sun hours per day. The exact number of sun hours is unknown but the graph shows that the investment will be paid back within a year with only 1.5 hours of sunshine per day.  When the solar plant pipings are insulated they will also be protected from rain. The evaporation of rain could be a great source of heat loss, not only during the rainy season but also during the dry season with frequent afternoon showers.

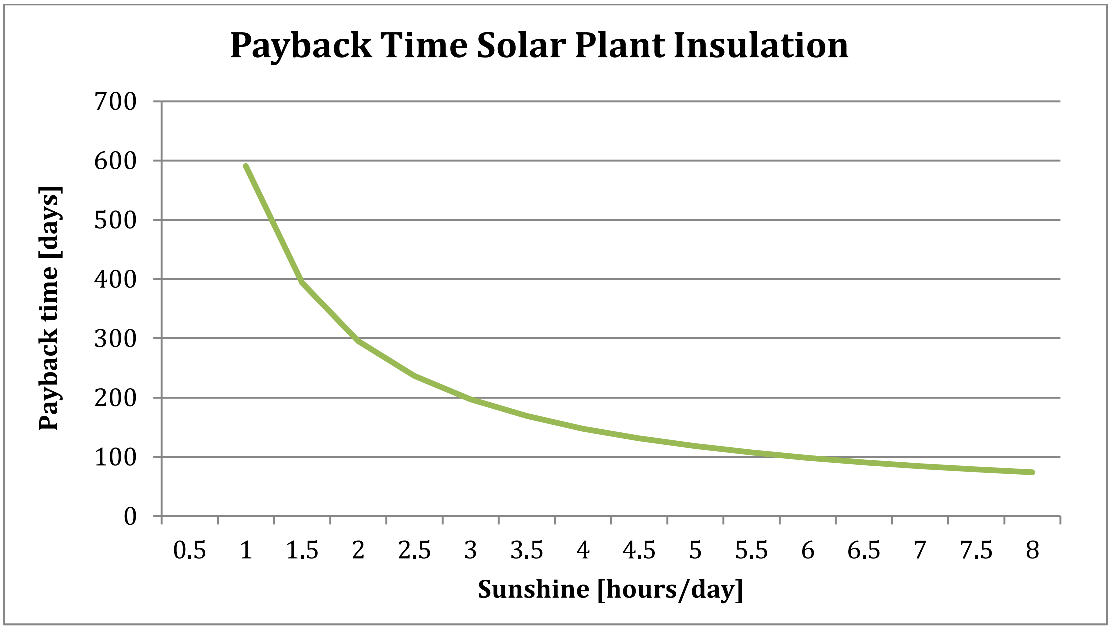


**Figure 8.6: Payback time for insulation of solar plant pipings**

Another source of efficiency reduction is that the panels are not clean, which can be seen figure 8.7. The area around the dryers' chimneys on the east side is the dirtiest.

**Figure 8.7: Dirty solar panels around the chimneys of the dryers on the east side of the roof**

Four circulation pumps are installed on the return pipes of the solar plant. That results in excessive pipings since the there are two return pipes per side instead of one. However, reconnecting the pipings and installing a new pump that can deliver the needed flow alone would probably not be profitable since the pump costs 7400 GHC (Blaser 2013). On the other hand the flow is only around 4 $m^3/h$ (chapter 7.7) which is far less than the flow estimation of 10.6 $m^3/h$ performed by the solar plant manufacturer (Junod 2013). The measurements showed that the supply temperature from the panels sometimes reached 90 °C (figure 7.7), i.e. above the dryer's optimal supply temperature. Furthermore, the efficiency of the panels decreases with increasing panel temperature (Junod 2013). One way of decreasing the supply temperature is to install a higher rated circulation pump. That could become increasingly important if the pipes are insulated and the panels are cleaned.

## 8.9 Storage Tank and Pipings

Two new connection boards are installed in the heat system, one for supply and one for return (figure 8.8). So far only dryer 4, the kerosene boiler and the storage tank are connected, but the plan is to connect all dryers and the biogas CHP in the near future. The idea is that the produced heat should supply the dryers directly without necessarily passing the storage tank. Since the tank is not dimensioned for the current flow rate or quantities of heat, overloading has been a problem (figure 7.6 and 7.7). Less mixing in the storage tank will give a better stratification and less thermal losses due to the lower average temperature. An additional measure that would avoid overloading of the storage tank is connection of the tank's temperature sensors to the kerosene boiler in order to automatically regulate the operation of the boiler.

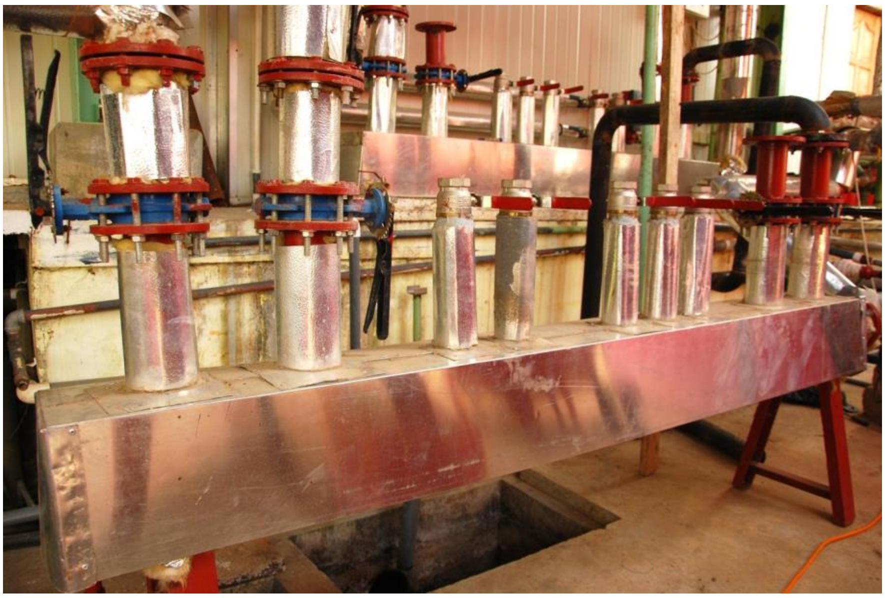

**Figure 8.8: Two new connection boards for the heat system, with return (atop) and supply**

The solar plant would benefit from a lower tank bottom temperature. The utilization would increase due to the larger temperature difference between the tank bottom and the solar plant supply. A reduced tank bottom temperature will also improve the cooling of the biogas CHP and increase the efficiency of the kerosene boiler.

At the moment there are some pipes in the heat system that are not insulated, mainly the ones of the solar plant and close to the storage tank. The latter will be solved when the new connection board is installed and the new piping for the dryers and the biogas CHP are insulated.

Boilers that are not in use or shut off are sources of heat losses because some heat enters from neighboring pipes with flowing water. To avoid these losses the boilers could be equipped with valves that are closed when the boiler is shut off.

## 8.10 PV Solar Plant

PV cells could be used to produce electricity as a complement to the diesel generator or ECG. Therefore the opportunity cost for both the diesel generator and ECG have been used to calculate the payback time for the installation of a PV solar plant, shown in figure 8.9 (equation 5.25, chapter 5.6.5). The resulting payback time is 4.5 years if the solar plant replaces the diesel generator and 6.8 years if replacing ECG.

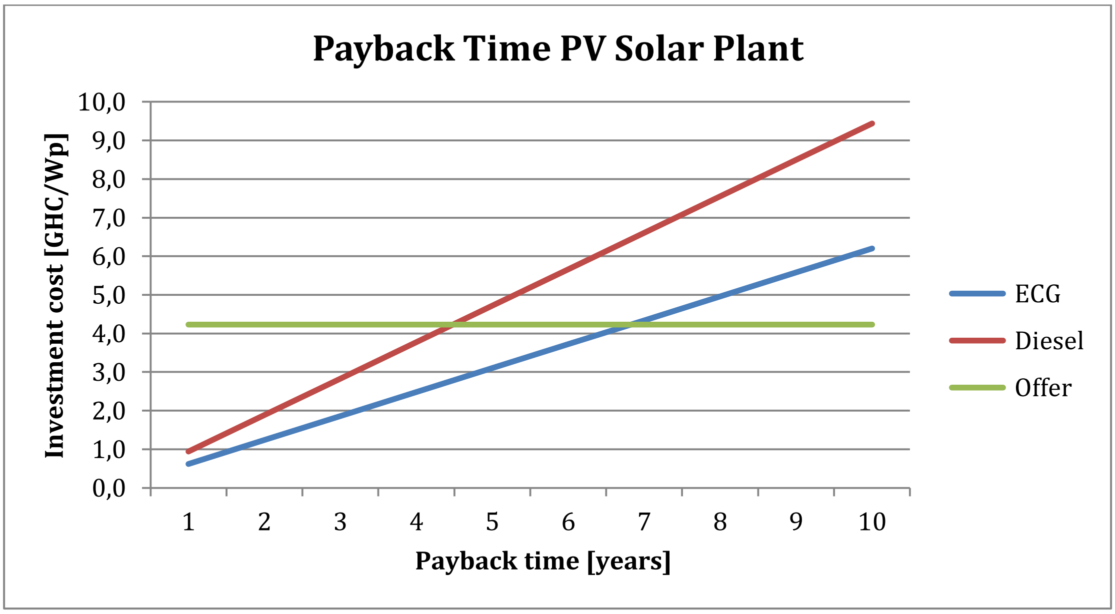


**Figure 8.9: Payback time for the purchase of a PV solar plant**

The PV plant can be connected to the grid, which means that the grid can be supplied by the plant if the power output exceeds the factory's loads. However, normally the output will be consumed directly since the installed power is 30 $kW_p$ and the factory's daytime average load is 87 kW (table 7.1). The exceeding power need of the factory in combination with the grid connection reduce the need of battery storage.

As mentioned in chapter 8.5, the future electricity production is difficult to foresee. Therefore it is uncertain how the electricity production from the PV cell plant will affect the usage of diesel and ECG. Nevertheless, a PV solar plant would decrease the factory's dependency on purchased energy and reduce its environmental impact.

# 9 Recommendations

HPW Fresh & Dry ltd. is recommended to:

(The recommendations are discussed in the chapter noted inside the parenthesis)

## 9.1 Heat

- Invest in new boilers for biogas and kerosene (8.6)
- Set aside the CHP and combust all the produced biogas in the new boiler (8.6)
- Consider direct heating with biogas if purchasing a new dryer (8.6)
- Invest in a roaster boiler for coconut shells (8.6)
- Connect all production and consumption units in the heat system, except for the solar plant, to the new connection board (8.9)
- Replace the heat exchangers in the heat recoveries of dryer 1-3 (8.3)
- Seal the exhaust outlets and insulate the pipes for the heat recovery of all dryers (8.3)
- Regulate the operation of boilers automatically by using temperature sensors connected to the heat storage tank, to avoid overloading of the tank (8.9)
- Insulate the solar plant pipings and clean the panels continuously (8.8)
- Replace the four circulation pumps of the solar plant with two larger and remove the surplus pipings at the same time (8.8)

## 9.2 Electricity

- Invest in a PV solar plant if the 5-7 years payback time is short enough (8.10)
- Balance the electrical loads Old factory and Overhead line (8.2)
- Reduce unnecessary use of motors for the biogas plant by training the technical staff (8.7)
- Install new evaporators in the general office, lab and local processing room and connect them to Bitzer tandem 2*10.8 A (8.4)
- Use Bitzer tandem 2*24.6 A to cool the new office, if it is not too far between the cooling machine and the office (8.4)
- Increase the amount of heat removed from the condenser of Bitzer tandem 2*24.6 A (8.4)
- Place all condensers shaded from the sun (8.4)
- Reduce the cooling need by shading and sealing doors and windows (8.4)

# 10 Future Work

In order to improve the factory's energy system further the following areas could be investigated:

- Efficiency of the fruit drying process, i.e. to improve the design of the dryers
- Increase of methane yield from the biogas plant
- Dimensioning, frequency regulation and soft starting of electric motors
- Automation of the heat producers in order to produce heat on demand
- Calculation of the benefit of installing a PV solar plant, with a more extensive analysis and an up-to-date offer

# 11 Reference List

## 11.1 Books

Alvarez, H. (2006). *Energiteknik del 1 och 2.* ISBN 978-91-44-04509-2 and 978-91-44-04510-8. Edition 3. Publisher: Studentlitteratur AB.

Nordling and Österman (2006). *Physics Handbook for Science and Engineering.* ISBN 978-91-44-04453-8. Edition 8:4. Publisher: Studentlitteratur AB.

Petchers, N. (2002). *Combined Heating, Cooling and Power Handbook – Technologies and Applications.* ISBN 978-08-24-74233-1. Publisher: The Fairmont Press.

Ragland, K., Bryden, K. (2011). *Combustion Engineering.* ISBN 978-1-4200-9250-9. Edition 2. Publisher: CRC Press.

## 11.2 Reports

Banzon, J. (1980). *The Coconut as a Renewable Energy Source.* Downloaded 01/25/2014 from: pcrdf.org/artimages%5Cart%203.doc

Blomström, H. (2013). *Effektiviseringspotential inom industrisektorn - Energibesparing vid frekvensstyrning av centrifugalpumpar - en fallstudie.* Downloaded 01/25/2014 from: http://uu.diva-portal.org/smash/get/diva2:646564/FULLTEXT02.pdf

Grim, J. and Johansson, M. (2012): *Evaluation of a biogas plant in Adeiso, Ghana.* Downloaded 01/25/2014 from: http://stud.epsilon.slu.se/5071/1/grim_j_johansson_m_121119.pdf

Shillings, C., Meyer, R., Trieb, F. (2004). *Solar and Wind Energy Resource Assessment (SWERA) - High Resolution Solar Radiation Assessment for Ghana.* Downloaded 01/25/2014 from: http://en.openei.org/datasets/files/710/pub/ghana_10km_solar_country_report.pdf

Stafell, I. (2011). *The Energy and Fuel Data Sheet.* Downloaded 01/25/2014 from: http://www.claverton-energy.com/wp-content/uploads/2012/08/the_energy_and_fuel_data_sheet.pdf

## 11.3 Data Sheets and Manuals

ABB (2011). *Vortez Flowmeter / Swirl Flowmeter FV4000 / FS4000 Operating Instructions D184B097U02.*

Bitzer (2012). *Condenser selection: Water-cooled Condensers, Type K573H.*

Dynameters (2012). *DMTFB/C Transit Time Ultrasonic Flow Meter Clamp-on & Insertion – Operation & maintenance manual*.

Guangdong Fivestar Solar Energy Co., Ltd. (2011). *Solar Collector Specification (FP3.0-A).*

HPW (2013). *Biogas recordings.*

Junod Wasser und Wärme AG (2013). *Prinzipschema Solaranlage Ghana.*

Olympian (2012). *GEP 165-1 Olympian Generator Sets.* Downloaded 01/26/2014 from: http://www.olympianpower.com/cda/files/2126429/7/LEHF0116-01.pdf

PCE Group (2013). *Manual PCE-UT232.*

RW De Beer & Associates (2010). *Quotation and contract document No. DRG/INT/1014/Q4.*

RW De Beer & Associates (2012). *Order confirmation contract document No. DRG/1014/Q8.*

## 11.4 Personal Communication

Blaser, M., Managing Director at HPW Fresh & Dry Ltd. Personal communication in Adeiso, October to December 2013.

Aklaku, E., Senior Lecturer at KNUST. Personal communication 11/25/2013 at KNUST in Kumasi.

Sundberg, C., Associate Professor at SLU. Personal communication via email January 2014.

# Appendix 1: Pictures from trainings

The pictures below show heat and electricity workshops with the technical staff.

# Appendix 2:
# Quick Start Guide Multimeter with Current Clamp

## Introduction

Before starting the measurements, make sure that you understand the following magnitudes:

- Voltage [**V**]. Voltage is the potential difference *between* two points.
- Current [**A**]. Current is the flow of electrons *through* a wire.
- Power [**kW**]. Power is the product of current and voltage. Power = Voltage · Current.
- Energy [**kWh**]. Energy is the product of power and time. Energy = Power · Time

## Measurements

The meter is started by pressing POWER.

### Line-to-neutral voltage of phase 1, 2 and 3

1. Attach a cord between the COM input terminal on the meter and the neutral of device that you want to measure.
2. Attach a cord between V1 input terminal on the meter and phase 1 of the device that you want to measure.
3. Repeat step 2 for phase 2 and 3.
4. Press MENU repeatedly until **V** is shown. Check that the voltage is around 220 V.
5. Press SELECT to select which phase to measure.

### Current of phase 1, 2 and 3

1. Put the clamp of the meter around the wire of phase 1. Make sure that only one wire is going through the clamp.
2. Press MENU repeatedly until **A** is shown. Read current.
3. Repeat step 1 for phase 2 and 3.

### Power of phase 1, 2 and 3

1. Go through step 1-5 of the voltage measurement instruction.
2. Do step 1 of the current measurement instruction.
3. Press MENU repeatedly until **kW** is shown. Read power.
4. Move the clamp to phase 2. Press SELECT to select phase 2.
5. Move the clamp to phase 3. Press SELECT to select phase 3.

### Energy of phase 1, 2 and 3

1. Go through step 1-5 of the voltage measurement instruction.
2. Do step 1 of the current measurement instruction.
3. Press MENU repeatedly until **kWh** is shown. The meter will count the amount of energy flowing through the wire until you remove the meter or until the current flow stops.
4. Move the clamp to phase 2. Press SELECT to select phase 2.
5. Move the clamp to phase 3. Press SELECT to select phase 3.
6. Press CLEAR if you want to restart the measurement (only in Active Energy mode).

### Saving and loading measurements

1. Press SAVE to store a screenshot. The meter can store up to 99 screenshots onto an internal memory.
2. Press LOAD to load the stored screenshots (cannot be done when measuring kWh).
3. Press CLEAR to remove *all* the stored screenshots from the memory (cannot be done when measuring kWh).

## Good to know

- The batteries last for 24 hours of measurements.
- Press LIGHT to turn the display backlight on for 30 seconds.
- Current measurements can be used to get a rough idea of the balance between the phases. However, keep in mind that the current is always varying because the load is always varying. To get a better picture, measure the energy consumed by each phase during a longer period by moving the meter between the phases every 30 minutes.
- To calculate the three phase power, sum up the power of the three phases.
  Three phase power = Power phase 1 + Power phase 2 + Power phase 3
- To calculate the three phase energy, sum up the energy consumed by the three phases.
  Three phase energy = Energy phase 1 + Energy phase 2 + Energy phase 3
- A three phase motor is balanced, i.e. the current through each phase is equal. When measuring a three phase motor, only one phase needs to be measured. There is no need to move the meter between the phases. The power of a three phase motor is equal to the power of one phase multiplied by 3. The energy consumption of a three phase motor is equal to the energy consumed by one phase multiplied by 3.

## Calculation examples

### Single phase power calculation

The energy consumed by a single phase machine during **2h:23min** of measurement was **6.7 kWh**.

Calculate the power need of the motor during the time of measurement.

**Solution**: The power can be calculated with the energy equation given in the introduction:

$$Energy\ [kWh] = Power[kW] * Time[h]$$

That gives:

$$Power\ [kW] = \frac{Energy\ [kWh]}{Time\ [h]}$$

The time must be converted to hours. 60 minutes is one hour. 23 minutes is $\frac{23}{60} = 0.38$ hours.

That gives **2h:23min = 2.38 h**.

Finally the power need of the motor can be calculated from:

$$Power = \frac{6.7\ kWh}{2.38\ h} = \mathbf{2.8\ kW}$$

### Three phase power calculation

The measured current from one phase of a three phase motor was **14 A**.

Calculate the three phase power of the motor during the time of measurement.

**Solution:** The power can be calculated with the power equation given in the introduction:

$$Power\ [W] = Voltage\ [V] * Current\ [A]$$

The line-to-neutral voltage can be assumed to be **220 V**. Remember that the three phase power of a balanced load is the single phase load multiplied by three.

That gives:

$$Power = 3 * 220\ V * 14\ A = 9240\ W \approx \mathbf{9.2\ kW}$$

## Current calculation

The rated power (wattage) of a single phase water boiler is **2 kW**.

Calculate how much current the water boiler will use.

**Solution:** The current can be calculated with the power equation given in the introduction:

$$Power\ [W] = Voltage\ [V] * Current\ [A]$$

That gives:

$$Current\ [A] = \frac{Power\ [W]}{Voltage\ [V]}$$

The line-to-neutral voltage can be assumed to be **220 V**.

The rated power was 2 kW which is equal to **2000 W** (If you use kW the answer will be in kA).

Finally the current of the water boiler can be calculated from:

$$Current = \frac{2000\ W}{220\ V} = \mathbf{9.1\ A}$$

# Appendix 3:
# Quick start guide – Heat energy meter
## Introduction

The heat energy meter is used to measure temperature difference and water flow in pipes without the need to drill or cut the pipe.

To measure flow, two transducers are used. The transducers can be mounted on either the supply or the return pipe, since the flow is the same.

To measure temperature difference, two temperature sensors are used. The sensors should be mounted on the supply and the return pipe.

Before starting the installation, think through what you want to measure. Locate where you have to install the equipment to achieve the purpose of your measurement.

Using temperature difference and flow, the thermal power can be calculated from:

Thermal power [kW]= 1.17 * Flow [$m^3$/h] * Temperature difference [°C]

## Mounting location

In order to get a good signal strength and quality, follow these advices when choosing your transducer mounting location:

- Make sure the pipe is completely filled with water, without air bubbles.
- Avoid pipes with vibrations.
- Make sure the transducers are mounted on a long enough stretch of straight pipe. Have at least ten pipe diameters (10D) of straight pipe upstream and five diameters (5D) downstream. If you are unsure, look at the figure below.
- Avoid shunts, valves and similar.

| Piping configuration<br>And transcducer position | Upstream Dimension<br>Pipe Diameters (*) | Downstream Dimension<br>Pipe Diameters (**) |
|---|---|---|
| 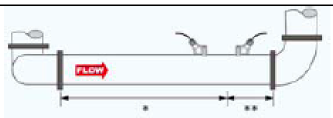 | 24 | 5 |
| 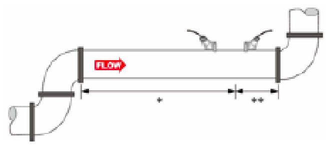 | 14 | 5 |
| 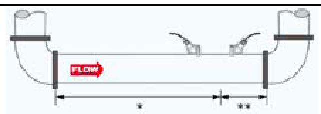 | 10 | 5 |
| 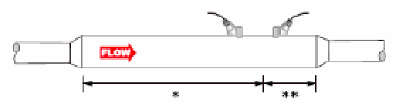 | 10 | 5 |
| 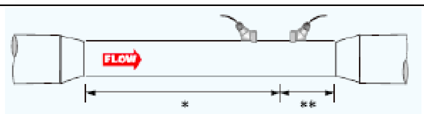 | 8 | 5 |
| 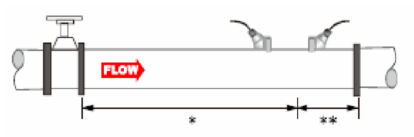 | 24 | 5 |

**Transducer position in different situations, seen from above.**

## Transducer spacing

Enter these parameters:

- **M11**: Outer diameter of the pipe
- **M12**: Wall thickness of pipe
- **M14**: Pipe material

The meter will give the transducer spacing in menu **M25**.

**Important**: These parameters have to be correct, otherwise the measurement will not be reliable.

## Pipe preparations

Clean the pipe from paint, rust and dirt. Make sure the pipe surface is smooth. Use the distance from menu **M25** to decide how big the cleaned spot has to be.

**Important**: For horizontal pipes: Mount the transducers in position 9 or 3 o'clock on the pipe (on the sides). Do not mount them on the top or bottom of the pipe, because that is where air and dirt gather.

## Mounting Transducers

There are three different mounting methods for the transducers. Use the V-method as standard, described in the figure below. To change method, use menu **M24**.

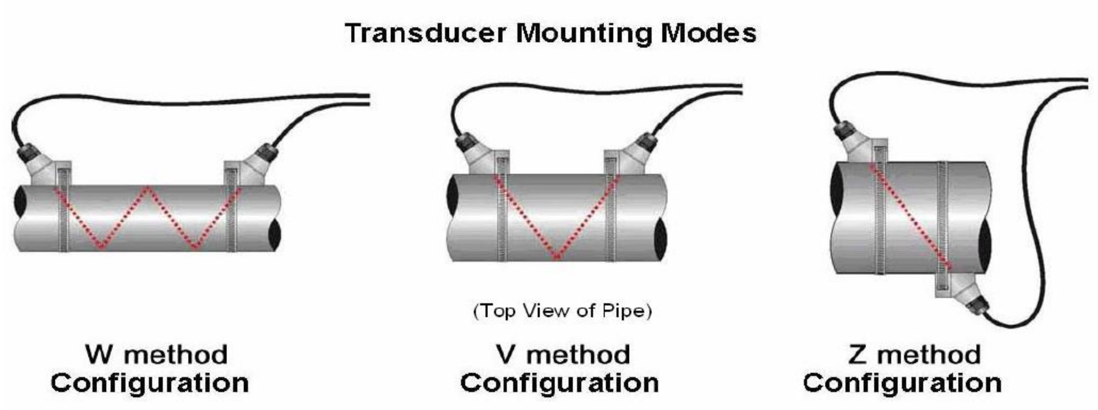


**Mounting methods for flow transducers.**

**Important**: The red transducer should be mounted upstream and the blue downstream in order to get the correct direction for the flow calculation.

Follow these steps when mounting the transducers:

1. Apply a thin layer of couplant grease on the contact area of the transducers.

2. Attach one transducer to the pipe with a steel strap and tighten the screw. Attach the other transducer a bit lose and change the distance between the transducers according to menu **M25**. **Important:** Do not tighten the screws too much since the (very expensive) transducers might crack.

3. Make sure that the transducers are in line and located 9 or 3 o'clock (on the sides).

4. Adjust the lose transducer with smooth movements and try to maximize the signal strength and signal quality in menu **M90**. For reliable measurement S and Q must be larger than 60.

5. Make sure that the Time Ratio, menu **M91**, is in the range 97-103 %

6. If possible, set zero flow in menu **M42** in order to remove offsets (static errors). **Important:** You have to be absolutely sure that the water is not moving before setting zero flow.

7. Check the flow in menu **M04**.

## Mounting temperature sensors

Follow these steps when mounting the temperature sensors:

1. Apply a thin layer of couplant grease on the surface of the sensor holder.

2. Attach the sensor holders on spots cleaned from paint, rust and dirt.

3. Put the sensors in the holders together with some couplant grease, and secure the sensors to the pipe with a wire. The red sensor should be mounted on the hot pipe and the blue on the cold pipe.

4. Insulate the sensor and the pipe with mineral wool, at least 30 cm on each side of the sensor.

5. Check the temperatures in menu **M06**.

## Important menus

The table below displays menus of interest.

| **Menu Window Number** | **Function/ Display** |
|---|---|
| M04 | Display the flow. [$m^3$/h] |
| M06 | Display Tin/Tout temperature value. [°C] |
| M11 | Window for entering outer diameter of the pipe. [mm] |
| M12 | Window for entering wall thickness. [mm] |
| M14 | Window for selecting pipe material.<br>0 = Carbon steel, 5 = PVC |
| M24 | Window for selecting transducer mounting method.<br>0 = V method |
| M25 | Display the transducer mounting spacing. [mm] |
| M42 | Set zero before the measurement, when the water is not moving. |
| M90 | Display signal strength (S) and quality (Q).<br>Let **S>60 and Q>60**. |
| M91 | Display the Time Ratio. The value should be in the range **97-103 %** |